Relatório de Atividades
"Jovem Talento (JTEE)"

FINDING A LINK BETWEEN THE FORMATION OF JOVIAN IRREGULAR SATELLITES AND OTHER DYNAMICAL CLASSES OF SOLAR SYSTEM MINOR BODIES

Dr. Gustavo Benedetti Rossi*
Supervisor: Dr. Ernesto Vieira Neto†
GRUPO DE DINÂMICA ORBITAL E PLANETOLOGIA

UNESP GUARATINGUETÁ
CAPES / PRINT - PROGRAMA INSTITUCIONAL DE INTERNACIONALIZAÇÃO
Processo 88887.571156/2020-00

Período Março/2021 a Maio/2023

*http://lattes.cnpq.br/1252286101311803
†http://lattes.cnpq.br/7161963144100182

Sumário

Resumo

O Modelo de Nice e suas modificações apresentam, em termos gerais, a história da formação e evolução do Sistema Solar (SS), onde interações entre os planetas gigantes e o disco de planetesimais primordial moldaram a estrutura dinâmica que observamos hoje. Entretanto, algumas classes dinâmicas - como a dos satélites irregulares dos planetas gigantes - ainda necessitam melhores explicações de sua origem, principalmente devido a novas descobertas e evidências observacionais. Esta população acredita-se ter sido capturada de diferentes famílias e grupos durante a história evolucional do SS. O estudo desta classe de objetos pode, então, fornecer restrições importantes sobre as condições nos modelos de formação do nosso sistema planetário.

Simulações numéricas apresentam boa concordância entre os números previstos e os satélites irregulares conhecidos dos planetas mais externos (principalmente Urano e Netuno). Em contrapartida, no caso de Júpiter ainda é necessário entender melhor os mecanismos de captura. Este trabalho apresenta um estudo destes mecanismos e evolução dos satélites irregulares jovianos através de simulações numéricas no contexto do Modelo de Nice e Jumping Jupiter. Seguindo procedimentos e implementações similares aos de (Izidoro et al., 2015, 2017) – e referências –, realizamos testes comparativos para validação do código, além de diversas simulações com diferentes números (e massa total) iniciais de super Terras, das quais selecionamos os melhores casos que reproduzem planetas similares a Urano e Netuno e analisamos os encontros próximos entre os gigantes. Aqui são apresentadas as atividades realizadas durante o período de bolsa, incluindo os resultados das mais de 23 mil simulações realizadas e suas implicações, publicado em (Benedetti-Rossi et al., 2023), trabalhos em colaboração e atividades de ensino e divulgação.

Abstract

The Nice Model and its modifications present, in general terms, the history of the formation and evolution of the solar system (SS), when interactions between giant planets and the primordial planetesimal disc shaped the dynamical structure that we observe today. However, some dynamical classes - such as the irregular satellites of the giant planets - still need better explanations about their origin, mostly due to new discoveries and observational evidences. This population is believed to be captured from different families and groups during the evolutional history of the SS. The study of this class of objects can then provide important constraints on the initial conditions for the models about the formation of our planetary system.

Numerical simulations present good agreement between the predicted number and the known irregular satellites for the outermost planets (mostly Uranus and Neptune). In contrast, for Jupiter it is still needed to better understand the capture mechanisms. This work present a study of those mechanisms and the evolution of the Jovian irregular satellites through numerical simulations on the context of the Nice Model and Jumping Jupiter. By following similar procedures and implementations to (Izidoro et al., 2015, 2017) – and references therein -, we performed comparative tests for the code validation, besides many simulations with different initial number (and total mass) of super Earths, from which we selected the best cases that reproduce planets similar to Uranus and Neptune, and we analyse the close encounters between the giant planets. Here it is presented the activities performed during the period as post-doc fellow, including the results from more than 23 thousand simulations and their implications, as published in (Benedetti-Rossi et al., 2023), as well as other works in collaboration and EPO activities.

1 Research Project

Aqui é apresentado o projeto, em inglês, como submetido para o pedido de bolsa.

1.1 Introduction

The formation and evolution of the solar system (SS) are well explained in general terms with the original Nice model (Tsiganis et al., 2005; Morbidelli et al., 2005) invoking a dynamical instability among the giant planets that was triggered by interaction with the primordial outer planetesimal disk (Levison et al., 2011; Nesvorný & Morbidelli, 2012). In this model, the migration and interaction of the giant planets in the early SS played a central role in shaping the dynamical structure of the present-day SS.

Many features of the outer SS configuration is explained in the Nice model, with supporting evidences such as the giant planet instability scenario explaining the capture of the Trojans asteroids of Jupiter and Neptune (Morbidelli et al., 2005; Nesvorný et al., 2013; Gomes & Nesvorný, 2016; Deienno et al., 2017), the existence of irregular satellites of the giant planets (Nesvorný et al., 2007, 2014) and the Kuiper belt's orbital structure (Nesvorný, 2015a,b; Nesvorný & Vokrouhlický, 2016; Gomes et al., 2018; Nesvorný, 2018; de Sousa et al., 2020). On the other hand, the inner SS presents a very complex structure that requires devoted attention to be better explained (Minton & Malhotra, 2009; Brasser et al., 2009; Walsh et al., 2011).

The two main reservoirs of small bodies, the Kuiper belt and the main asteroid belt, provide important constraints on the planetary evolution. While the the Kuiper belt specially provides hints on the evolution of giant planets' migration, the outermost region of the main asteroid belt is a witness of the past evolution of Jupiter. Other interesting populations of objects are the Trojans, Hildas and the Centaurs.

Jupiter Trojans are the population of minor bodies in the same orbit as the planet, lying 60° ahead of the planet in its orbit or 60° behind, in the Lagrangean points L4 and L5, respectively. The Hildas' population orbits the sun in the 3/2 Jovian mean-motion resonance. Simulations have shown that the primordial populations in those regions were first emptied during the period in which Jupiter and Saturn crossed a mean-motion resonance, and then replaced with planetesimals scattered inward from the region beyond the ice giants (Gomes et al., 2005; Morbidelli et al., 2005; Roig & Nesvorný, 2015). The Centaurs are minor bodies with orbital semi-major axis between Jupiter and Neptune (between 5 and 31 astronomical units (au)). Since they are crossing the orbit of one or more giant planets, they suffer strong gravitational perturbations which make their orbits very unstable, with dynamic lifetimes of only a few million years (Horner et al., 2004), and so it is believed that this population did not form on this region of the solar system, but once belonged to the trans-Neptunian region and were scattered to their present orbits (Lykawka & Mukai, 2008; Parker, 2015; Santos-Sanz et al., 2016).

The irregular satellites of the giant planets also present interesting features and an orbital history and evolution not yet fully understood, despite many and extensive efforts. Jupiter's irregular moons orbit the planet far enough that the precession of their orbital plane is primarily controlled by the Sun (Burns & Matthews, 1986). They can also present prograde and retrograde orbits, with tightly clustered orbits (Nesvorný et al., 2003; Sheppard & Jewitt, 2003) which origin could be from disruptive collisions between asteroids or large moons or even captured from different populations (from the outer main belt, Trojans, Hildas, or the Centaurs (Sheppard, 2005; Nesvorný et al., 2007, 2014)). Due to these irregular orbits, they are believed to have formed outside the circumplanetary accretion and are likely products of early capture from heliocentric orbit. The irregular satellites may be the only small bodies remaining which are still relatively near their formation locations within the giant planet region (Sheppard, 2005).

Other ways to obtain more constraints about the origin and orbital evolution of the irregular satellites is through the study of their astrometric position and their physical characteristics. Considering the Jupiter's irregular moons, since most of them are too small (with km-size), they are very hard to observe and some of them get lost and need to be rediscovered (Brozović & Jacobson, 2017). Long-term astrometric observations can help understand their current orbit and its evolution. Brozović & Jacobson (2017) also showed that the current data set appears to be sensitive to the mass of Himalia, which leads us to take a look into their physical characteristics. According to Nesvorný et al. (2003) some of the satellites were formed through collisions between them, such as Himalia, Elara, Lysithea and Leda. Those objects were studied by Grav et al. (2003) and their color (B - V = 0.66 ± 0.02 and V - R = 0.36 ± 0.01) are very similar to C-type asteroids. This similarity was confirmed by Bhatt et al. (2017), showing that those satellites are very likely to be formed in the main belt. Other groups of objects with very high orbital inclination, such as Pasiphae and Ananke groups present present different colors than the main object: while Pasiphae shows a similarity with C-type asteroids, Megaclite and Callirrhoe for example, have similarities with P or D-type asteroids. In the case of Ananke, the opposite happens, it is similar to P or D-type asteroids while member of the cluster such as Harpalyke, Praxidike and Iocaste are more like C-type (Grav et al., 2003). In the retrograde group, where Carme and Taygete are present, some objects such as Kalyke are very red, suggesting a common origin with Centaurs or TNOs.

In this context, knowing about the physical characteristics, origins and orbital evolution of the Jovian irregular satellites can give us hints about the formation of the SS and put or improve the constraints on the models. In this project we intend to compare their properties with the some of the main belt objects, besides the Hildas, Trojans, Centaurs and families in the outer main belt to evaluate their similarities and/or differences and thereby empirically test current dynamical instability models. By comparing their physical properties and analysing their orbital evolution we could find links between them and put constraints on SS formation and evolution models.

1.2 Statement of the problem

One of the long-standing problems for the dynamical evolution of the Solar System concerns the initial mass distribution of the protoplanetary nebula that evolved to the observed population in the solar system. Understanding each population of objects through their physical and dynamical characteristics can give important information for constraining those formation and evolution models. The Jupiter irregular satellites present a wide range of characteristics, both orbital and physical, indicating that they may have been captured from different populations in the solar system in different evolutionary epochs.

In this project we propose to analyse the physical characteristics, orbital configuration and evolution of many irregular satellites of Jupiter, using state-of-the-art numerical simulations and the current paradigm of giant planet formation and dynamical evolution in the Solar System, improving the results from previous work we can seek answers to some questions, among them:

- What are the most-likely origins of the Jovian irregular satellites? What family or dynamical group they belong?
- How and when did the capture happened? What were the main processes involved? What were the dynamical influences on other satellites during capture? For how long do they last in those orbits? Can they migrate into a more regular orbit, and how long does it take?
- Is it possible that they formed *in-situ* and after some close encounter with a satellite (or between Jupiter and other giant) they migrated to the current orbit? Are they (and how much) similar/-different from other satellites in the same region? Are they (and how much) similar/different from the regular satellites?
- How similar are their physical characteristics to other solar system populations (outer main belt, centaurs, TNOs, Hildas, Trojans, etc)?
- Could they provide a link to other populations in order to constrain the history and evolution of the solar system?

1.3 Methodology

We will perform numerical simulations for the formation and evolution of the Solar System and invoke a new and self-consistent approach compared to previous studies. Our simulations will include a primordial planetesimal disk that will interact with the giant planets and growing ice giants during the gas disk phase. During the gas disk phase, we will also take into account the gas drag and gas dynamical friction effects on planetesimals (Brasser et al., 2007; Grishin & Perets, 2015).

To perform the simulations we will use the REBOUND N-body integrator[1] due to its very flexible and customized programming to accurately and efficiently solve many problems in astrophysics. To run the simulations the "Grupo de Dinâmica Orbital e Planetologia" counts on a computer cluster prepared and optimized for numerical calculations. In the present configuration it is available more than 220 processors, 80 Gb of RAM, and 10 Tb for data storage. The cluster also counts with 2 workstations equiped with 2 GPUs each for massively parallelized calculations. If necessary, we can submit a request for processing time at the Santos Dumont supercomputer, located at Laboratório Nacional de Computação Científica (LNCC)[2]. It counts on 34.688 cores distributes in 1132 computing nodes with a capacity of 5,1 Petaflop/s

[1] https://rebound.readthedocs.io/en/latest/

[2] https://sdumont.lncc.br/machine.php?pg=machine

($5,1 \cdot 10^{15}$ float-point operations per second). It is also possible to acquire processing time from comercial solutions through resources from the FAPESP project "A relevância dos pequenos corpos em dinâmica orbital" (16/24561-0).

We also intend to ask for telescope time at Observatório Pico dos Dias (OPD) in order to obtain new astrometric positions for the irregular satellites and combine them with past observations that the Rio Group may have in the database, as well as participate in collaboration with ongoing project by Dr. Altair R. Gomes-Junior with the ongoing project "Caracterização de Satélites Irregulares através de Ocultações Estelares e curva de rotação". Considering that Jupiter is still close to the galactic plane, the characteristics of the irregular satellites, and the available equipment at OPD, it is possible to observe objects with limit apparent magnitude of approximately 20.5, translating into ∼15 km Jovian satellite.

1.4 Expected Results

The main result expected is the confirmation of the origin of the irregular satellites from other dynamical classes of minor bodies in the solar system (outer main belt, Trijans, Hildas, Centaurs and TNOs). We also intend to better constrain the epoch and time span that the capture happened. This can input constraints for minor bodies on solar system formation models, such as the initial mass, number of particles, formation regions, migration times, among others.

We also expect to confirm and verify the existence of family of objects and constrain the orbital characteristics for a specific population and family through correlations and metrics (see for example Carruba & Michtchenko (2007, 2009); Carruba et al. (2013, 2019)).

A secondary possible result, that will depend on new observations and long-term analysis, is to obtain astrometric positions for the irregular satellites, improving their orbits and ephemeris.

References

Benedetti-Rossi, G., Ribeiro, R., Winter, O. C., Gaspar, H. S., Vieira-Neto, E. (2023). Accretion of ice giant planets from massive protoplanets whose migration is blocked by Jupiter and Saturn. *MNRAS* 526, 4435–4454. http://doi.org/10.1093/mnras/stad3017

Bhatt, M., Reddy, V., Cloutis, E., et al. (2017). Composition of Jupiter irregular satellites sheds light on their origin. *A&A*, 608:A67

Brasser, R., Duncan, M. J., and Levison, H. F. (2007). Embedded star clusters and the formation of the Oort cloud. II. The effect of the primordial solar nebula. *Icarus*, 191:413–433.

Brasser R., Morbidelli A., Gomes R., Tsiganis K., Levison H. F., (2009). Constructing the secular architecture of the solar system II: the terrestrial planets. *A&A*, 507:1053

Brasser, R.; Morbidelli, A., (2013). Oort cloud and Scattered Disc formation during a late dynamical instability in the Solar System. *Icarus*, V. 225, Issue 1, p. 40-49.

Brozović, M. and Jacobson, R. A., (2017). The Orbits of Jupiter's Irregular Satellites. *AJ*, V. 153, Number 4

Burns, Joseph A.; Matthews, Mildred Shapley (1986). Satellites. Satellites by Joseph A. Burns and Mildred Shapley Matthews. University of Arizona Press, 1986. ISBN: 978-0-8165-0983-6

Carruba, V. and Michtchenko, T. A., (2007). A frequency approach to identifying asteroid families. *A&A* 475, 1145–1158

Carruba, V. and Michtchenko, T. A., (2009). A frequency approach to identifying asteroid families II. Families interacting with nonlinear secular resonances and low-order mean-motion resonances *A&A* 493, 267–282

Carruba, V., Domingos, R. C., Nesvorný, D., Roig, F., Huaman, M. E., Souami, D., (2013). A multidomain approach to asteroid families' identification. *MNRAS*, V. 433, Issue 3, Pages 2075–2096

Carruba, V., Aljbaae, S., Lucchini, A., de Oliveira, E. R., (2019). Machine learning identification of asteroid families. *EPSC-DPS Joint Meeting 2019*, Vol. 13, EPSC-DPS2019-130-2

Cresswell, P.; Nelson, R. P. (2008). Three-dimensional simulations of multiple protoplanets embedded in a protostellar disc. *A&A*, V. 482, Issue 2, 2008, pp.677-690

Deienno, R., Morbidelli, A., Gomes, R. S., and Nesvorný, D. (2017). Constraining the Giant Planets' Initial Configuration from Their Evolution: Implications for the Timing of the Planetary Instability. *AJ*, 153:153.

Gaspar, H. S. (2013). Origem dos satélites irregulares de Júpiter: Captura de asteroides binários primordiais. *Tese de doutorado*, FEG/UNESP - Guaratinguetá

Gomes, R.; Levison, H. F.; Tsiganis, K.; Morbidelli, A. (2005). Origin of the cataclysmic Late Heavy Bombardment period of the terrestrial planets. *Nature*, V. 435, Issue 7041, pp. 466-469

Gomes, R. and Nesvorný, D. (2016). Neptune trojan formation during planetary instability and migration. *A&A*, 592:A146.

Gomes, R., Nesvorný, D., Morbidelli, A., Deienno, R., and Nogueira, E. (2018). Checking the compatibility of the cold Kuiper belt with a planetary instability migration model. *Icarus*, 306:319–327.

Gomes-Júnior A. R., Morgado B. E., Benedetti-Rossi G., Boufleur R. C., Rommel F. L., Banda-Huarca M. V., Kilic Y., Braga-Ribas, F. and Sicardy, B. (2022), *MNRAS*, 511, 1167.

Grav, T., Holman, M. J., Gladman, B. J., and Aksnes, K. (2003). Photometric survey of the irregular satellites. *Icarus*, 166(1):33–45.

Grav, T., Bauer, J. M., Mainzer, A. K., Masiero, J. R., Nugent, C. R., Cutri, R. M., Sonnett, S., and Krame, E., (2015). NEOWISE: Observations of the irregular satellites of Jupiter and Saturn. *AJ*, V. 809, Number 1

Grishin, E. and Perets, H. B. (2015). Application of Gas Dynamical Friction for Planetesimals. I. Evolution of Single Planetesimals. *ApJ*, 811:54.

Holt, T. R.; Brown, A. J.; Nesvorný, D.; Horner, J.; Carter, B. (2018). Cladistical Analysis of the Jovian and Saturnian Satellite Systems *AJ*, V. 859, Issue 2.

Horner, J.; Evans, N. W.; Bailey, M. E. (2004), Simulations of the population of Centaurs - I. The bulk statistics. *MNRAS*, 354, 798-810

Izidoro, A.; Morbidelli, A.; Raymond, S. N.; Hersant, F.; Pierens, A. (2015). Accretion of Uranus and Neptune from inward-migrating planetary embryos blocked by Jupiter and Saturn. *A&A*, V. 582, id.A99

Izidoro, A.; Ogihara, M.; Raymond, S. N.; Morbidelli, A.; Pierens, A.; Bitsch, B.; Cossou, C.; Hersant, F. (2017). Breaking the chains: hot super-Earth systems from migration and disruption of compact resonant chains. *MNRAS*, V. 470, Issue 2, 1750-1770

Kroupa, P., Aarseth, S., and Hurley, J. (2001). The formation of a bound star cluster: from the Orion nebula cluster to the Pleiades. *MNRAS*, 321(4):699–712.

Kokubo, E. and Ida, S. (2000). Formation of Protoplanets from Planetesimals in the Solar Nebula. *Icarus* v. 143, Issue 1, p. 15-27,

Levison, H. F., Morbidelli, A., Tsiganis, K., Nesvorný, D., and Gomes, R. (2011). Late Orbital Instabilities in the Outer Planets Induced by Interaction with a Self-gravitating Planetesimal Disk. *AJ*, 142:152.

Lykawka, P. S.; Mukai, T. (2008), The intrinsic Neptune Trojan orbit distribution: Implications for the primordial disk and planet migration. *AJ*, 135, 4, 1161-1200

Minton D. A., Malhotra R. (2009). A record of planet migration in the main asteroid belt. *Nature*, 457:1109

Morbidelli, A., Levison, H. F., Tsiganis, K., and Gomes, R. (2005). Chaotic capture of Jupiter's Trojan asteroids in the early Solar System. *Nature*, 435:462–465.

Nesvorný, D.; Alvarellos, J. L. A.; Dones, L.; Levison, H. F. (2003) Orbital and Collisional Evolution of the Irregular Satellites. *AJ*, V. 126, Issue 1, pp. 398-429.

Nesvorný, D., Vokrouhlický, D., and Morbidelli, A. (2007). Capture of Irregular Satellites during Planetary Encounters. *AJ*, 133:1962–1976.

Nesvorný, D. and Morbidelli, A. (2012). Statistical Study of the Early Solar System's Instability with Four, Five, and Six Giant Planets. *AJ*, 144:117.

Nesvorný, D., Vokrouhlický, D., and Morbidelli, A. (2013). Capture of Trojans by Jumping Jupiter. *ApJ*, 768:45.

Nesvorný, D., Vokrouhlický, D., and Deienno, R. (2014). Capture of Irregular Satellites at Jupiter. *ApJ*, 784:22.

Nesvorný, D. (2015a). Evidence for Slow Migration of Neptune from the Inclination Distribution of Kuiper Belt Objects. *AJ*, 150:73.

Nesvorný, D. (2015b). Jumping Neptune Can Explain the Kuiper Belt Kernel. *AJ*, 150:68.

Nesvorný, D. and Vokrouhlický, D. (2016). Neptune's Orbital Migration Was Grainy, Not Smooth. *ApJ*, 825:94.

Nesvorný, D. (2018). Dynamical Evolution of the Early Solar System. *ARA&A*, 56:137–174.

Parker, A. H. (2015), The intrinsic Neptune Trojan orbit distribution: Implications for the primordial disk and planet migration. *Icarus*, 247, 112-125

Papaloizou, J. C. B.; Larwood, J. D. (2000). On the orbital evolution and growth of protoplanets embedded in a gaseous disc *MNRAS*, V. 315, Issue 4, 823-833

Papaloizou, J. C. B. (2020) Oxford Research Encyclopedia of Planetary Science. Edited by Peter Read et al. ISBN: 978-0-190-64792-6. Oxford University Press, 2020, id.190

Roig, F. and Nesvorný, D. (2015). The evolution of asteroids in the jumping-Jupiter migration model. *AJ*, 150:186 (15pp)

Santos-Sanz, P.; French, R. G.; Pinilla-Alonso, N.; et al. (2016), James Webb Space Telescope Observations of Stellar Occultations by Solar System Bodies and Rings. *PASP*, 128, 959, 018011

Sheppard, S. S.; Jewitt, D. C. (2003). An abundant population of small irregular satellites around Jupiter. *Nature*, V. 423, Issue 6937, pp. 261-263.

Sheppard, S. S., (2005). Outer irregular satellites of the planets and their relationship with asteroids, comets and Kuiper Belt objects. *Proceedings of the International Astronomical Union*, 1(S229), 319-334

Sheppard, S. S.; Williams, G. V.; Tholen, D. J.; Trujillo, C. A.; Brozovic, M.; Thirouin, A.; Devogele, M.; Fohring, D.; Jacobson, R.; Moskovitz, N. A., (2018). New Jupiter Satellites and Moon-Moon Collisions. *Research Notes of the American Astronomical Society*, V. 2, Issue 3, article id. 155, (2018).

de Sousa, R. R., Morbidelli, A., Raymond, S. N., Izidoro, A., Gomes, R. and Vieira Neto, E. (2020). Dynamical evidence for an early giant planet instability. *Icarus*, 339:113605.

Stone, Lukas R.; Kaib, N. A. (2021) Evolution of primordial Kuiper belt binaries through a giant planet instability. *MNRAS Letters*, V. 505, Issue 1, pp.L31-L35

Tsiganis, K., Gomes, R., Morbidelli, A., and Levison, H. F. (2005). Origin of the orbital architecture of the giant planets of the Solar System. *Nature*, 435:459–461.

Walsh K. J., Morbidelli A., Raymond S. N., O'Brien D. P., Mandell A. M., (2011). A low mass for Mars from Jupiter's early gas-driven migration. *Nature*, 475:206

2 Research Project Schedule

Table 1 presents the intended schedule for the project.

2.1 Relevance of the Project

This work is self-consistent and uses recent approaches and observational constraints of the current models solar system formation in order to study the origin and evolution of irregular Jovian satellites, helping to understand the planet migration and interactions between the planets and minor bodies in the early history of the solar system.

My expertise in Astronomical Observations and my know-how with programming and data reduction, specially with photometry and astrometry, will be very relevant to complement the expertise in dynamical formation of planets and satellites of the "Grupo de Dinâmica Orbital e Planetologia da UNESP", given crucial contributions to the group, and also given me new expertise to my formation.

2.2 The relevance of the project in CAPES-PrInt program

This projects fits well within the main theme "Ciencia básica na fronteira do conhecimento" in the CAPES-PrInt program. The project goals fit in the thematic of Theme 7 in a study of the complex systems (Objective number 5) and the planetary systems are directly involved on it. We emphasize that our project applies to i) scientific computation; ii) nonlinear dynamics; (iii) dynamical systems.

2.3 Our project to international and national networks

The project will be hosted at Sao Paulo State University (Unesp) which is the host institution of the "Grupo de Dinâmica Orbital e Planetologia" (GDOP).

The GDOP and I have an ongoing collaboration with the "Rio Group" – with researchers from Observatório Nacional (ON/MCTIC), Observatório do Valongo (OV/UFRJ), and Universidade Tecnológica Federal do Paraná (DAFIS/UTFPR) – and the "European Research Council - Lucky Star[3]", lead by Dr. Bruno Sicardy from the Observatoire de Paris-Meudon in France, where I have a post-doc position at the present moment.

I am affiliated to the Laboratório Nacional de e-Astronomia (LIneA) where we develop tools for data analysis in the big data era (such as DES and LSST). I have also collaboration with many professional and citizen scientists (amateurs) from all around the world due to the stellar occultation project, as well as a collaboration with the RECON project leaders Marc Buie and John Keller from the Southwest Research Institute (SwRI) in the US.

The supervisor has also ongoing collaboration with Dr. Renner from Université de Lille, France, Dr. Morbidelli from Observatoire de la Côte d'Azur, France, Dr. Kley from Universität Tübingen, Germany.

The project presented here will increase and reinforce those ongoing collaborations.

3 Plan of Teaching and Academic activities

3.1 Teaching

I have a vast observational experience with more than 200 nights in the past 10 years operating the 3 telescopes at the Observatório do Pico dos Dias (OPD/LNA) in both presential and remotely modes and using different optical instruments. Science cases in the observations are mostly astrometry and photometry, with applications in stellar occultations, rotational light curves, satellites mutual approximation, and mutual phenomenon. In all those cases I have also large experience in data reduction and analysis with the development of softwares and routines in fortran and python 3.

My teaching experience for post-graduation students counts on one semester classes for a discipline given at Observatório Nacional (Tópicos de Ocultações Estelares). I also have a 1.5 year experience in teaching Physics and Mathematics for elementary and high school students.

The host institution of the project provides the possibility to minister classes about Astronomy and celestial mechanics. I intend to give one discipline during the 12 months period of the CAPES-PRINT program. I can offer the following proposed discipline (to be approved by the post-graduation program)[4]:

- **Name**: Técnicas observacionais e redução de dados astronômicos
- **Program**:

[3] https://lesia.obspm.fr/lucky-star/index.php

[4] The approval of new disciplines requires a discussion of the discipline program and adaptations to the requisites and pre-requisites of the students and the institution interests.

- Técnicas observacionais: Astrometria, Fotometria, Espectroscopia, Radioastronomia, Interferometria;
- Conceitos observacionais: Telescópio, Sistemas de referência, Catálogos, Filtros, Sinal, Ruído, SNR, PSF, Seeing, Escala de placa, raios cósmicos, magnitude, paralaxe, movimento próprio, entre outros;
- Imagens de Calibração: Bias, Dark, Flat-Field;
- Aplicações em Ocultações, Aproximações, Fenômenos Mútuos, Curvas de luz de rotação;

- **Recommended Bibliography**:

  Conceitos de Astronomia - Roberto Boczko (Ed. Edgard Blücher 1984)

  Spherical Astronomy - R.M. Green, 1985.

  Reference Frames in Astronomy and Geophysic - J. Kovalesky, I.I. Mueler & B. Kolaczek ed., Kluwer Academic Publishers, 1988;

  Very Long Baseline Interferometer - F. Takahashi, T. Kondo, Y. Takahashi & Y. Koyama, Ohmsha Press, 2000;

  Astrometry of Fundamental Catalogues - H.G. Walter & O.J Sovers, SpringerVerlag ed., 2000;

  Eletronic Imaging in Astronomy - Ian McLean, Springer 2008;

  Handbook of CCD Astronomy - STEVE B. HOWELL, National Optical Astronomy Observatory and WIYN Observatory, Cambridge Univ. Press, 2006

  Fundamental Astronomy - H. Karttunenm P. Kröger, H. Oja, M. Poutanen, K. J. Donner, Springer 1987

  An Introduction to Astronomical Photometry Using CCDs - W. Romanishin, University of Oklahoma, 2006

  Artigos especializados

- **Suplementary Bibliography**:

  The Hipparcos and Tycho Catalogues, vol I, II, III - SP-1200, 1997;

  Vectorial Astronomy - C.A. Murray, 1983.

  Spherical Astronomy - R.M. Green, Cambridge University Press, 1985;

  Planetary Sciences - Imke de Pater, Jack J. Lissauer, Cambridge Univ. Press, 2007

3.2 Students and orientation

I co-oriented one master student in 2018 (orientation by Julio I. B. Camargo) with his dissertation entitled "*Astrometria de objetos Transnetunianos e Centauros na era Gaia: posições a partir de imageamento direto e de ocultção estelar*", and oriented one "Iniciação Científica" student during 2 years with projects entitled "Fotometria e obtenção de curva de luz com dados de ocultações estelares através do uso de diferentes softwares" and "Estudo de períodos rotacionais de objetos Transnetunianos"

Due to the short period of the CAPES-PRINT program, it is not possible to become an advisor for a PhD thesis, but I will be able to co-advise any student in collaboration with some of the permanent personnel in the department. I will also be available to advise any student in a master program or in the "Iniciação Científica" program with subjects related to the institution interests.

3.3 EPO activities

I have participated in many Education and Public Outreach (EPO) activities with special attention to the "Semana Nacional de Ciência e Tecnologia" in 2018 at Observatório Nacional, the participation in the program "Skype a Scientist" with online seminars in english, spanish and french for 8-13 years students, and some invited seminars and webinars for elementary schools in Itatiba-SP, Pindamonhagaba-SP, and Valinhos-SP.

The institution has an observatory installation equipped with a telescope and a scientific camera and already offers various Education and Public Outreach (EPO) activities during the year, with a spotlight on the "Asteroid Day" program on June 30th. I intend to continue my participation in those activities, as well as to participate and propose, during the year, activities and seminars for the general public.

Tabela 1: Project Schedule

Year	1 (Mar/2021 - Fev/2022)												2 (Mar/2022 - Fev/2023)												3 (Mar-Mai/2023)		
Month	01	02	03	04	05	06	07	08	09	10	11	12	13	14	15	16	17	18	19	20	21	22	23	24	25	26	27
Literature review and analysis																											
Model adaptation and programming																											
Model and code verification																											
Simulation runs																											
Observation* (astrometry)																											
Data analysis																											
Data Publication (Submission)																											
Reports																											
Teaching**																											
Student advising and EPO activities																											

Notes: * Observations will depend on time proposal acceptance at OPD, as well as good conditions of observation. Observations can also be obtained with the ongoing collaboration with the "Rio Group". ** Teaching period is intended (but not limited) for two semesters and will depend on the schedule and bureaucracy of the PG program.

4 Relatório de Atividades

As atividades propostas para o projeto estão apresentadas na Tabela 1. Todas foram realizadas, com pequenas variações e adaptações de acordo com as dificuldades e desafios enfrentados durante a execução do projeto, como descrito nas seções a seguir. Uma apresentação geral das atividades realizadas neste projeto está nas Seções 4.1, 4.2, 4.3 e 4.4 e o resultado completo deste trabalho está na publicação Benedetti-Rossi et al. (2023) (apresentado no Apêndice A). As atividades de observação estão apresentadas na Sec. 4.5 e as de ensino, pesquisa e extensão estão descritas na Seção 4.6, enquanto outros trabalhos e atividades desenvolvidas em colaborações estão apresentadas na Seção 4.7.

4.1 Revisão e análise de artigos

A primeira tarefa proposta foi a revisão de vários artigos sobre a formação e evolução do Sistema Solar e a análise detalhada dos métodos e equações. Dentre eles, merecem destaque alguns artigos dos quais foram baseados modelos, equações, condições iniciais das simulações numéricas, entre outros parâmetros. São eles: Holt et al. (2018), Nesvorný et al. (2003, 2007, 2014), Izidoro et al. (2015, 2017), Cresswell & Nelson (2008), Papaloizou & Larwood (2000), Papaloizou (2020), Stone & Kaib (2020) e Gaspar (2013)

Durante a revisão foram encontrados alguns erros em algumas das equações, que foram corrigidas posteriormente na adaptação dos nossos modelos e programação.

4.2 Adaptação dos modelos e programação

Nesta segunda tarefa, foram realizadas reuniões semanais para discussão do direcionamento do projeto, das dificuldades com a implementação e verificação dos códigos e outros detalhes necessários para o bom andamento do desenvolvimento do projeto, bem como realizada a análise detalhada das equações para implementação.

Além das reuniões, foi realizada a instalação, familiarização e testes com o Rebound em linguagens python e C, e a instalação e testes do programa Mesquite (para a parte de cladística). Para acompanhamento e versionamento do programa, foi criado um repositório no GitHub com o código de integração numérica (Rebound).

Seguindo os procedimentos em Nesvorný et al. (2007, 2014); Izidoro et al. (2015, 2017) (e referências citadas), implementamos nos códigos de simulação numérica de N-corpos (Rebound) as equações para o perfil de densidade superficial (x), gradiente de temperatura (β), e torques do gás sofridos por um planeta com migração tipo-I (Γ_{Tot}) – que incluem as contribuições dos torques de Lindblad (Γ_L) e Co-rotacional (Γ_C) – que atuam sob os efeitos da difusão térmica e viscosa do gás. Também foram incluídos os efeitos do amortecimento em excentricidades e inclinações e suas acelerações, além das equações para as escalas de tempo de migrações e os processos de adição de massa após um encontro entre 2 corpos.

Muitas simulações foram realizadas para verificar os resultados com os resultados apresentados nos artigos usados (como citados na seção 4.1). É importante ressaltar que foi necessário muitas horas de verificação dos códigos para encontrar erros nas equações apresentadas nos artigos (*typos*, sinais invertidos, entre outros), além da modelagem do cenário adaptado no nosso programa.

4.3 Simulações numéricas - programação, validação e execução

A terceira tarefa proposta compete a programação, validação e execução dos códigos e está intimamente ligada às tarefas apresentadas na Sec. 4.4. Para otimização dos procedimentos e bom andamento do desenvolvimento do projeto, foram realizadas reuniões semanais para discussão do direcionamento, das dificuldades com a implementação e verificação dos códigos e outros detalhes necessários.

O procedimento padrão inclui em linhas gerais a implementação do código, sua execução considerando vários parâmetros iniciais, a análise geral, a adaptação e seleção de parâmetros mais adequados, a execução de várias simulações com os parâmetros escolhidos, a análise e comparação com os resultados da literatura, a escolha de melhores parâmetros, e finalmente a execução em grande número para a análise estatística final.

As implementações iniciais foram realizadas e validadas no primeiro semestre, quando foi criado e adaptado uma rotina para executar o programa diversas vezes com parâmetros sendo escolhidos aleatoriamente conforme o apresentado nos artigos citados na Sec. 4.2. Vários parâmetros foram testados e adaptados, de acordo com o apresentado na bibliografia e modificados para implementar a qualidade do trabalho, conforme também às exigências do *referee* do artigo publicado.

Como já mencionado, foi usado o Rebound para realizar as simulações numéricas de N-corpos dos embriões planetários interagindo com o Sol, Júpiter, Saturno e o gás do disco protoplanetário. As simulações foram realizadas usando um integrador híbrido do MERCURIUS, usando um passo de tempo inicial de 0,5 anos.

Entre as simulações relevantes, as quais foram executadas em grande número e posteriormente publicadas, foram preparadas 72 configurações iniciais para as simulações. Elas são obtidas combinando diferentes massas totais iniciais do disco (30, 45, 50 ou 60 $M_\oplus$) divididas igualmente entre o número inicial de embriões (2, 3, 5, 10, 15 ou 20). Esses valores foram escolhidos para investigar a formação de protoplanetas que podem atingir tamanhos similares a Urano e Netuno. Além disso, em cada uma destas configurações, Júpiter e Saturno foram posicionados, respectivamente, em órbitas circulares em (i) 5,0 e 6,55 au, correspondente a um sistema mais compacto (TI), e (ii) 5,4 e 7,076 au, correspondente a um sistema mais espalhado (WI).

Nas simulações foram usadas um controle orbital para Júpiter e Saturno que imita os efeitos da migração tipo II (Cresswell & Nelson, 2008). Desta forma, os embriões planetários interagem com os dois gigantes, enquanto que Júpiter e Saturno sofrem apenas pequenas mudanças em suas órbitas devido à pequena massa individual dos embriões.

Os embriões planetários foram inicialmente posicionados conforme o seguinte procedimento: é primeiramente calculado o raio de Hill de Saturno e depois adicionado o raio de Hill do embrião calculado à distância heliocêntrica de Saturno, multiplicado por um fator aleatório entre 5 e 10. Os embriões seguintes são colocados da mesma maneira, adicionando o raio de Hill calculado na órbita do anterior e multiplicado por um fator aleatório entre 5 e 10. Isso foi importante, pois a formação de embriões planetários por acreção de cascalho tipicamente cria uma separação estável entre os vizinhos por um fator de 5 raios de Hill (Kokubo & Ida, 2000).

Todas as inclinações e excentricidades dos embriões foram ajustadas para 0,001 e 0,01, respectivamente, e os outros parâmetros orbitais foram selecionados aleatoriamente. Finalmente, para completar as 72 configurações, simulações foram executadas com um tempo total de dissipação do gás de 2, 3, 5 e 9 milhões de anos (Myr). Para cada uma das 18 configurações com 5 Myr foram executadas 1000 simulações, enquanto que para as outras foram executadas 100 simulações, totalizando 23400 simulações, que ocuparam um total de mais de 930Gb de espaço em disco com um tempo de execução aproximadamente de 96 horas (executadas em um computador pessoal core I5 9th Gen, com 8 núcleos).

4.4 Simulações numéricas - análise de dados e resultados

As tarefas propostas nesta atividade está intimamente ligada às atividades da Sec. 4.3, e são realizadas em ciclos de programação, análise, reprogramação, reanálise, etc., até chegar em resultados que são satisfatórios.

Assim que foram iniciadas as análises, foi notado que havia um erro no código, pois várias simulações causavam erro de segmentação. Após diversas tentativas e verificações, foi encontrado um problema nas equações do torque no modelo de Izidoro et al. (2017), então foi utilizado apenas a equação do torque total de Izidoro et al. (2015).

Outro problema encontrado inicialmente foi que na maioria das simulações, Júpiter e Saturno migravam muito para o Sistema Solar interior, com Júpiter chegando a ficar com semi-eixo maior igual a 1 ua em muitas simulações (em menos de 5 milhões de anos). Investigando o que foi feito por Izidoro em seus trabalhos, nota-se que houve um posicionamento forçado para os dois gigantes. Por isso, fizemos alguns testes para analisar e contornar tal comportamento. Primeiramente consideramos um sistema somente com Júpiter e Saturno e dois ou três embriões com 15 massas da Terra cada em ressonância de movimento médio, mas as migrações e interações foram satisfatórias somente quando não se considerava o gás nas simulações. Passamos então a considerar um sistema somente com os dois gigantes, que também não produziu resultados satisfatórios com a presença do gás. Uma terceira tentativa pensada foi de implementar forças de amortecimento nos semi-eixos e excentricidades da órbita dos gigantes, mas a implementação destas forças não é trivial e ocuparia grande parte do tempo para desenvolver as equações e implementação no código. Por isso, foi decidido deixar Júpiter e Saturno em órbitas circulares fixas e deixado essa implementação para um trabalho futuro.

Além do problema da migração indesejada dos gigantes, notamos também que os embriões estavam sendo colocados muito afastados ao considerar uma distância de 5 a 10 raios de Hill mútuos, com embriões chegando em algumas simulações a mais de 150 ua. Observando as figuras dos trabalhos de Izidoro, vimos que os espaçamentos considerados não era o raio de Hill mútuo, mas sim apenas o raio de Hill do último embrião.

Após todas as verificações e análises preliminares, reiniciamos as simulações para cada caso com as novas considerações e um tempo de vida do gás de 5 Myr. Destas simulações, notamos que muitos dos sistemas se tornam estáveis, geralmente presos em cadeias de ressonância de movimento médio (MMRs), com pouquíssimas interações. Assim, a maioria das interações acontece nos primeiros 2 a 3 Mys. Baseado nesses resultados, executamos simulações em menor número (100 ao invés de 1000) para 2, 3 e 9 Myr. Isso porque com 2 a 3 Myr, em geral, não há tempo suficiente para o sistema formar as cadeias de MMRs, como notado por Izidoro et al. (2015). Para 9 Myr, o sistema já atinge as cadeias e realizamos para verificação de possíveis eventos após os 5 Myr.

No fim, após a seleção dos melhores parâmetros e casos, foram realizadas 23400 simulações em 72 configurações. Notamos que em todos os casos, a maior parte das interações próximas (CE) entre os embriões e os planetas gigantes ocorre nos primeiros 1,5 Myr, independentemente do tempo de vida do gás. Raras fusões, ejeções ou interações fortes entre os objetos ocorrem após 4 Myr. Em geral, há poucas diferenças entre as configurações TI e WI. Uma característica típica das simulações é o alto número de encontros próximos com os planetas gigantes (aproximadamente 2000 por simulação). Além disso, alguns embriões planetários "pulam" para órbitas internas à de Júpiter, entrando no Sistema Solar interno ou sobrevivem em MMR 1:1, ficando coorbital com Júpiter. No final da fase de gás, tipicamente somente 2 ou 3 planetesimais sobrevivem, mesmo em simulações com altos números iniciais de embriões.

A análise completa dos resultados está apresentada em Benedetti-Rossi et al. (2023).

4.5 Realização de observações

As observações servem como um complemento para a análise numérica apresentada nas seções anteriores. Além disso, encaixa em projetos de colaboração para análise astrométrica, fenômenos mútuos dos satélites dos planetas gigantes, além de ocultações estelares.

As observações são, em geral, realizadas remotamente no Observatório do Pico dos Dias (OPD/LNA). Foram realizadas observações nos dias 26 de Março, 27 de Abril, 16 de Maio, 19 e 30 de Junho, 31 Julho, 05 e 27 Agosto, 18 de Setembro, 08 de Novembro, 02 de Dezembro de 2021, 05 de Maio, 29 de Junho, 07 e 23 de Julho, 01 e 20 de Agosto, 05, 12 e 13 de Setembro, 17 de Outubro, 21 de Novembro e 04 de Dezembro de 2022, 18 de Abril e 10 de Maio de 2023.

Realizei também a redução e análise astrométrica de observações realizadas com aquisição de dados nos dias 05, 06 e 07 de Maio; 03, 04, 05, 18, 19, 20, 24, 29 e 30 de Setembro, 02, 07 e 21 de Outubro, 05, 06, 07 e 27 de Novembro de 2021; 26 de Março; 09, 10, 24, 27 de Abril; 10, 11, 14 e 17 de Maio; 11, 16, 17, 18, 30 de Junho; 4, 12, 13, 17, 27, 29, 30, 31 de Julho; 01, 05, 06, 07, 16, 22 e 31 de Agosto de 2022.

Além do OPD, também preparei e submeti um pedido de tempo de observação para os telescópios Gemini Norte e Sul para uma ocultação estelar por Netuno em outubro de 2021, que foi aceito e concedido 2.5 horas no Gemini Norte e 1.5 horas no Gemini Sul. Estas observações foram realizadas na noite de 7 de Outubro de 2021, e os dados ainda estão em análise.

4.6 Atividades de ensino e divulgação

Durante o período da bolsa, participei em conjunto com o Prof. Dr. Rafael Sfair ministrando as aulas da disciplina de "Introdução à Astronomia Fundamental" na graduação FEG-UNESP com carga horária de 4 horas semanal, além da disciplina "Astronomia Observacional" com carga horária de 90 horas. Vale destacar a participação como membro suplente da defesa de qualificação da aluna Vanessa Maria Francisco de Moura no dia 11/Agosto/2021 às 10h e como membro externo da banca de seleção de trabalhos de Iniciação Científica do Observatório Nacional (em 13/08 e 19/08).

Além do ensino formal, participei também de diversas atividades de divulgação científica. Entre as atividades realizadas estão:

- Preparação de vídeos para o canal de divulgação do canal no YouTube do GDOP/UNESP[5];
- Organização e elaboração de regulamento do "Concurso de Desenho" para o "Asteroid day" (realizado no canal do Youtube do GDOP/UNESP em 30 de junho de 2021);
- Organização e elaboração de regulamento do I Festival de poesia do GDOP para o "Dia internacional de observação da Lua" (realizado no canal GDOP/UNESP em 16 de outubro de 2021);

[5] https://www.youtube.com/channel/UC-8eTKrfxzta1M6EDoyVY2g

- Organização e participação nos eventos de divulgação do GDOP ("Asteroid Day" em 2021 e 2022, "Dia internacional de observação da Lua" em 2021, "Dia dos detritos espaciais" em 2022 e 2023, e "Escola de Verão" em 2023;
- Transmissões ao vivo no canal do YouTube do GDOP na série "Bate-papo GDOP"
- Transmissões ao vivo no canal do YouTube dos **AstroTubers**[6] sobre diversos temas relacionados à Astronomia;
- Seminários de divulgação para alunos de escola pública e privada;

4.6.1 Atividades GDOP/UNESP

Anualmente são realizadas 4 atividades principais no GDOP/UNESP: "Dia internacional de observação da Lua", "Dia dos detritos espaciais", "Escola de Verão" e "Asteroid Day".

A **noite internacional de Observação da Lua** (International Observe the Moon Night) é um momento para se reunir com colegas entusiastas da Lua e pessoas curiosas por todo o mundo. Todos na Terra estão convidados a aprender mais sobre a ciência e a exploração da Lua, fazer parte de observações celestes, e honrar conexões culturais e pessoais com a Lua. Note que nós encorajamos você a interpretar "Observação" de forma ampla. O International Observe the Moon Night ocorre anualmente em setembro ou outubro, quando a Lua está em quarto crescente – uma ótima fase para uma noite de observação.

Em 2021 também realizamos um Festival de Poesias com o tema A Lua, aberto ao público em geral de todas as idades. No dia 16 de outubro de 2021, durante o evento, apresentamos as 15 poesias selecionadas. Para cada poesia foi produzido um vídeo com a respectiva declamação do próprio autor. Os vídeos com a declamação podem ser encontrados no canal do YouTube do GDOP. Além das 15 poesias selecionadas, outras 24 poesias foram consideradas de destaque pelo júri e foram convidadas para compor um Livro Eletrônico, que permanecerá na página web do GDOP. O Livro do I FESTIVAL DE POESIA do GDOP contém as poesias, bem como, os links para o vídeo de declamação de cada uma delas.

Toda a organização do evento, tanto da transmissão ao vivo quanto ao concurso de poesias, foi feito por professores e pós-graduandos do GDOP. O vídeo do evento pode ser encontrado no link https://www.youtube.com/watch?v=p_nPG7tSs3s e o livro digital com as poesias podem ser encontradas no link https://www.dinamicaorbital.org/livro-digital-i-festival-de-poesias/.

Em 10 de fevereiro de 2009, o satélite Iridium 33 colidiu com o satélite Cosmos 2251, a primeira e única colisão entre dois satélites intactos da nossa era de exploração espacial, até agora. Essa colisão aconteceu a uma velocidade de mais de 40 mil km/h e gerou uma nuvem de destroços no ambiente espacial da Terra. Os destroços desta colisão juntamente com outros lixos que orbitam a Terra são chamados de detritos espaciais. O Space Debris Day – **Dia dos Detritos Espaciais** marca o aniversário desta colisão e é feito para criar um alerta sobre a grande ameaça que os detritos espaciais podem representar para o nosso dia-a-dia. Em 2022, o evento foi realizado no dia 22 de fevereiro de 2022 e no dia 11 de fevereiro de 2023 em transmissão ao vivo no canal do YouTube do GDOP com palestras de pesquisadores da UNESP/FEG.

Toda a organização do evento, tanto da transmissão ao vivo quanto ao concurso de poesias em 2022, foi feito por professores e pós-graduandos do GDOP. Os vídeos do evento podem ser encontrados nos links https://www.youtube.com/watch?v=4Ow1ExTSBtw e também https://www.youtube.com/watch?v=UTAZzvuZK_M.

A **Escola de verão** (http://escola.dinamicaorbital.org/) é oferecida anualmente pelo Grupo de Dinâmica Orbital e Planetologia da FEG/UNESP (GDOP) e tem como público alvo professores, graduados e graduandos na área de ciências exatas, incluindo alunos de cursos de licenciatura. O objetivo do evento é a difusão e divulgação de conceitos básicos e temas atuais da área de pesquisa, contribuindo com a formação dos alunos, facilitando o contato com pesquisadores na área de astronomia e astronáutica e observando a aplicação de conceitos matemáticos e físicos aprendidos em aula nas atividades científicas atuais. Espera-se também que a Escola faça parte no processo de atualização do conhecimento dos professores da região, oferecendo um ganho de conteúdo nas aulas de Física e Ciências nas escolas das quais os professores participarem da Escola de verão. Participei da edição de 2023 como palestrante e como monitor do observatório.

O **Dia do Asteroide**, ou *Asteroid Day*, é um evento mundial que ocorre sempre no dia 30 de Junho, data em que foi registrado o evento de Tunguska na Sibéria, em 1908. A proposta deste evento é informar sobre a importância do estudo de asteroides e o que pode ser feito para proteger o planeta no caso de um impacto. No GDOP, realiza-se desde 2017 um evento totalmente gratuito e para o

[6] https://www.youtube.com/c/AstroTubers

público de todas as idades. O evento conta com palestras, exposições, atividades e visitas ao observatório do departamento. Eu participo da organização do evento desde 2021, que foi realizado virtualmente excepcionalmente (o vídeo pode ser encontrado na parte de transmissões ao vivo do canal do GDOP no YouTube - https://www.youtube.com/@gdopunesp9500).

4.6.2 Canal GDOP/UNESP e Observatório

Durante o estágio de pós-doutoramento na Faculdade de Engenharia e Ciências de Guaratinguetá da UNESP (FEG/UNESP), entre 2021 a 2023, participei da organização e execução de várias atividades já consolidadas no Grupo de Dinâmica Orbital e Planetologia (GDOP). O departamento conta com um observatório equipado com um telescópio Meade de 16", e realiza atividades de visitas para observação de objetos no céu. Participei de dezenas de noites de observação, recebendo mais de uma centena de visitantes ao longo do período do meu estágio, entre 2021 e 2023. Além das atividades de observação, a equipe do GDOP também organiza um seminário virtual, chamado "**Bate-papo GDOP**" em que uma pessoa do departamento apresenta os resultados de uma de suas publicações mais recentes. O bate-papo acontece no canal do YouTube do departamento (https://www.youtube.com/@gdopunesp9500) e conta com 13 edições.

4.6.3 Canal Astrotubers

Em 2017, durante a XLI reunião anual da Sociedade Astronômica Brasileira (SAB), vários astrônomos mostraram interesse em fazer uma divulgação científica de qualidade. Então, junto com alguns mestrandos e doutorandos nos unimos para criar um canal no YouTube. Posteriormente, no ano de 2018, esse canal deu origem ao **AstroTubers** (https://www.youtube.com/astrotubers), que passou por diversas atualizações e modificações com entradas e saídas de colaboradores. Particularmente, entrei oficialmente no canal em 2021 e hoje somos 5 graduados e pós-graduados de física e de astronomia de diversas universidades do Brasil. O **AstroTubers** visa realizar divulgação de física, astronomia e outros assuntos "*nerd*" que possuem algum tópico de astronomia e conta hoje com quase 90 mil inscritos. Publicamos vídeos toda terça-feira e fazemos transmissões ao vivo quase semanalmente às quarta-feiras, onde convidamos pesquisadores, mestrandos e doutorandos de várias áreas da astronomia para um bate-papo com os ouvintes e seguidores do canal. Dentre as transmissões ao vivo, fui responsável pela organização e criação de conteúdo de mais de 140 delas. Também apresentamos conteúdo na rede social *Instagram* (https://www.instagram.com/astrotubers - com mais de 9 mil inscritos), e publicamos frequentemente em outras redes sociais. O canal AstroTubers possui seu conteúdo certificado pela SAB (http://bit.ly/SeloSAB) e detém o selo SVBR, *Science Vlogs Brasil* (http://bit.ly/ScienceVlogsBrasil), que atesta a qualidade da divulgação científica no YouTube.

4.6.4 Outras Atividades de Divulgação

Além das atividades como organizador, tive outras participações em transmissões ao vivo como convidado. Os eventos foram:

- Planetário de São Paulo - 24/03/2022 - Pequenos Corpos do Sistema Solar https://www.youtube.com/watch?v=y0eGXyif-Go
- Canal com Q - 29/03/2022 - O que é Astronomia? O que faz um astrônomo? https://www.youtube.com/watch?v=I1hLUjyPa6Q

Também participei, junto a outros colegas, de um evento chamado "Esquenta OBA" realizado pelo Instituto Nossa Senhora do Carmo em Guaratinguetá-SP. O evento foi uma preparação para alunos de ensino fundamental do quinto e sexto anos escolares que têm intenção de participar da Olimpíada Brasileira de Astronomia (OBA). Foi então preparado algumas atividades como a observação da Lua em um telescópio, palestras e reconhecimento do céu utilizando o aplicativo *Stellarium*. Além disso, ministrei palestras gratuitas em escolas públicas e privadas na cidade de Itatiba-SP.

4.7 Outros Trabalhos de Colaboração

Além das atividades previstas no cronograma, realizei diversas outras atividades relacionadas à pesquisa, desenvolvimento científico, colaborações em trabalhos e participação em eventos científicos.

O trabalho em colaboração com pesquisadores do ON e LIneA para o desenvolvimento de uma interface gráfica para o SORA (Stellar Occultation Reduction and Analysis (Gomes-Júnior et al., 2022)), submetido ao Heising-Simons Foundation, vinculado ao LSST, foi aceito e recebi o valor de 20 mil USD. O projeto teve início em janeiro, quando foi realizado o cronograma, aberto o chamado para empresas de tecnologia apresentarem propostas de participação e também contratado dois alunos de iniciação científica. Os alunos aprenderam os processos científicos relacionados às ocultações estelares e desenvolveram um manual de uso para o programa, além de auxiliar a criação da documentação. O programa "OccultIn" teve sua versão final (v0.96) apresentada com resultados satisfatórios para uma primeira análise. Entretanto, não ficou suficientemente pronta para uma versão que possa ser publicada e utilizada por pesquisadores e comunidade amadora.

Participei também como membro de uma banca avaliadora de trabalhos de jovens cientistas no Colégio Visconde de Porto Seguro - Valinhos no dia 06/Novembro/2021 e de uma banca avaliadora de trabalhos de iniciação científica do Observatório Nacional nos dias 08 e 09 de Dezembro/2021.

Iniciei minha participação como membro avaliador de pedidos de tempo dos telescópios GEMIINI, organizado pelo Laboratório Nacional de Astrofísica, da qual faço parte até hoje. Nesta comissão, os pedidos de tempo são analisados, classificados para discussão entre os membros, discutindo seus méritos, e depois reclassificados para distribuição de tempo.

Também, como projeto em desenvolvimento paralelamente, foram reduzidas e analisadas curvas de luz de várias ocultações estelares por diversos objetos do Sistema Solar.

4.7.1 Eventos (Reuniões e Congressos)

No período da bolsa participei de algumas reuniões, encontros e congressos, com apresentação de trabalho, com participação como co-autor de trabalhos ou como participante, como listado abaixo:

- XLIV Reunião Anual da Sociedade Astronômica Brasileira (ReASAB) - 13 a 17 de Setembro de 2021 - autor principal de 1 trabalho e co-autor de outros 11 trabalhos `https://sab-astro.org.br/eventos/reuniao-anual-da-sab/eventos-anteriores/xliv-reuniao-anual-da-sab/`;
- Europlanet Science Congress 2021 - participação e co-autoria de trabalhos
- "Lucky Star webmeeting" - 03, 04, 07 e 08 de Junho/2021 - participação
- Colóquio Brasileiro de Dinâmica Orbital 2020/21 (CBDO) - 06 a 10 de Dezembro de 2021 - autor de 2 trabalhos e co autor de outros trabalhos `https://sites.google.com/site/2020cbdo/xx-col%C3%B3quio-brasileiro-de-din%C3%A2mica-orbital-cbdo-2020`;
- LSST Brazil 2021 - 07 e 08 de Dezembro de 2021 - Participação `https://lsst-brazil2021.linea.gov.br/`;
- XI Taller de Ciencias Planetarias - 14 a 18 de Fevereiro de 2022 - autor de 1 trabalho e co-autor de outros trabalhos `http://gcpsj.sdf-eu.org/tcp-2022/tcp-2022.html`;

4.7.2 Publicações

O trabalho principal deste projeto foi publicado na revista "MNRAS" Benedetti-Rossi et al. (2023), no qual fui primeiro autor, mas a colaboração em outros trabalhos também teve ótimos resultados, com a minha coautoria nas seguintes publicações:

- Benedetti-Rossi et al. 2023: BENEDETTI-ROSSI, G; RIBEIRO, R ; WINTER, O C ; GASPAR, H S ; VIEIRA-NETO, E . Accretion of ice giant planets from massive protoplanets whose migration is blocked by Jupiter and Saturn. MONTHLY NOTICES OF THE ROYAL ASTRONOMICAL SOCIETY, v. 526, p. 4435-4454, 2023
- Morgado et al. 2021: MORGADO, B. E. ; SICARDY, B. ; Braga-Ribas, F. ; DESMARS, J. ; GOMES-JÚNIOR, A. R. ; BÉRARD, D. ; LEIVA, R. ; Ortiz, J. L. ; VIEIRA-MARTINS, R. ; BENEDETTI-ROSSI, G. ; SANTOS-SANZ, P. ; CAMARGO, J. I. B. ; Duffard, R. ; ROMMEL, F. L. ; ASSAFIN, M. ; BOUFLEUR, R. C. ; COLAS, F. ; KRETLOW, M. ; BEISKER, W. ; Sfair, R. ; et.al . Refined physical parameters for Chariklo's body and rings from stellar occultations observed between 2013 and 2020. ASTRONOMY & ASTROPHYSICS, v. 652, p. A141, 2021

- Santos-Sanz et al. 2021: SANTOS-SANZ, P. ; Ortiz, J. L. ; SICARDY, B. ; POPESCU, M. ; BENEDETTI-ROSSI, G. ; MORALES, N. ; VARA-LUBIANO, M. ; CAMARGO, J. I. B. ; PEREIRA, C. L. ; ROMMEL, F. L. ; ASSAFIN, M. ; DESMARS, J. ; Braga-Ribas, F. ; Duffard, R. ; MARQUES OLIVEIRA, J. ; VIEIRA-MARTINS, R. ; FERNÁNDEZ-VALENZUELA, E. ; MORGADO, B. E. ; ACAR, M. ; ANGHEL, S. ; et.al . Physical properties of the trans-Neptunian object (38628) Huya from a multi-chord stellar occultation. ASTRONOMY & ASTROPHYSICS, v. 664, p. A130, 2022

- Sicardy et al. 2021: SICARDY, BRUNO ; ASHOK, NAGARHALLI M. ; TEJ, ANANDMAYEE ; PAWAR, GANESH ; DESHMUKH, SHISHIR ; DESHPANDE, AMEYA ; SHARMA, SAURABH ; DESMARS, JOSSELIN ; ASSAFIN, MARCELO ; ORTIZ, JOSE LUIS ; BENEDETTI-ROSSI, GUSTAVO ; BRAGA-RIBAS, FELIPE ; VIEIRA-MARTINS, ROBERTO ; SANTOS-SANZ, PABLO ; CHAND, KRISHAN ; BHATT, BHUWAN C. . Pluto?s Atmosphere in Plateau Phase Since 2015 from a Stellar Occultation at Devasthal. The Astrophysical Journal, v. 923, p. L31, 2021.

- Gomes-Júnior et al 2022: GOMES-JÚNIOR, A R ; MORGADO, B E ; BENEDETTI-ROSSI, G ; BOUFLEUR, R C ; ROMMEL, F L ; BANDA-HUARCA, M V ; KILIC, Y ; BRAGA-RIBAS, F ; SICARDY, B . SORA: Stellar occultation reduction and analysis. ROYAL ASTRONOMICAL SOCIETY. MONTHLY NOTICES, v. 511, p. 1167-1181, 2022

- Marques-Oliveira et al. 2022: MARQUES OLIVEIRA, J. ; SICARDY, B. ; GOMES-JÚNIOR, A. R. ; Ortiz, J. L. ; STROBEL, D. F. ; BERTRAND, T. ; FORGET, F. ; LELLOUCH, E. ; DESMARS, J. ; BÉRARD, D. ; DORESSOUNDIRAM, A. ; Lecacheux, J. ; LEIVA, R. ; MEZA, E. ; ROQUES, F. ; SOUAMI, D. ; WIDEMANN, T. ; SANTOS-SANZ, P. ; MORALES, N. ; BENEDETTI-ROSSI, G. ; et.al . Constraints on the structure and seasonal variations of Triton?s atmosphere from the 5 October 2017 stellar occultation and previous observations. ASTRONOMY & ASTROPHYSICS, v. 659, p. A136, 2022.

- Santos-Sanz et al. 2022: SANTOS-SANZ, P. ; Ortiz, J. L. ; SICARDY, B. ; POPESCU, M. ; BENEDETTI-ROSSI, G. ; MORALES, N. ; VARA-LUBIANO, M. ; CAMARGO, J. I. B. ; PEREIRA, C. L. ; ROMMEL, F. L. ; ASSAFIN, M. ; DESMARS, J. ; Braga-Ribas, F. ; Duffard, R. ; MARQUES OLIVEIRA, J. ; VIEIRA-MARTINS, R. ; FERNÁNDEZ-VALENZUELA, E. ; MORGADO, B. E. ; ACAR, M. ; ANGHEL, S. ; et.al . Physical properties of the trans-Neptunian object (38628) Huya from a multi-chord stellar occultation. ASTRONOMY & ASTROPHYSICS, v. 664, p. A130, 2022.

- Vara-Lubiano et al. 2022: VARA-LUBIANO, M. ; BENEDETTI-ROSSI, G. ; SANTOS-SANZ, P. ; Ortiz, J. L. ; SICARDY, B. ; POPESCU, M. ; MORALES, N. ; ROMMEL, F. L. ; MORGADO, B. ; PEREIRA, C. L. ; ÁLVAREZ-CANDAL, A. ; FERNÁNDEZ-VALENZUELA, E. ; ILIC, D. ; VINCE, O. ; BACHEV, R. ; SEMKOV, E. ; NEDELCU, D. A. ; ¸SONKA, A. ; HUDIN, L. ; BOACA, M. ; et.al . The multichord stellar occultation on 2019 October 22 by the trans-Neptunian Object (84922) 2003 VS2. ASTRONOMY & ASTROPHYSICS, v. 663, p. A121, 2022.

- Assafin et al. 2023: ASSAFIN, M ; SANTOS-FILHO, S ; MORGADO, B E ; GOMES-JÚNIOR, A R ; SICARDY, B ; MARGOTI, G ; BENEDETTI-ROSSI, G ; BRAGA-RIBAS, F ; LAIDLER, T ; CAMARGO, J I B ; VIEIRA-MARTINS, R ; SWIFT, T ; DUNHAM, D ; GEORGE, T ; BARDECKER, J ; ANDERSON, C ; NOLTHENIUS, R ; BENDER, K ; VISCOME, G ; OESPER, D ; et.al . Kilometer-precise (UII) Umbriel physical properties from the multichord stellar occultation on 2020 September 21. MONTHLY NOTICES OF THE ROYAL ASTRONOMICAL SOCIETY, v. 526, p. 6193-6204, 2023.

- Fernández-Valenzuela et al. 2023: FERNÁNDEZ-VALENZUELA, E. ; MORALES, N. ; VARA-LUBIANO, M. ; Ortiz, J. L. ; BENEDETTI-ROSSI, G. ; SICARDY, B. ; KRETLOW, M. ; SANTOS-SANZ, P. ; MORGADO, B. ; SOUAMI, D. ; ORGANERO, F. ; ANA, L. ; FONSECA, F. ; ROMÁN, A. ; ALONSO, S. ; GONÇALVES, R. ; FERREIRA, M. ; IGLESIAS-MARZOA, R. ; LAMADRID, J. L. ; ALVAREZ-CANDAL, A. ; et.al . The multichord stellar occultation by the centaur Bienor on January 11, 2019. ASTRONOMY & ASTROPHYSICS, v. 669, p. A112, 2023

- Morgado et al. 2023: MORGADO, B. E. ; SICARDY, B. ; Braga-Ribas, F. ; Ortiz, J. L. ; SALO, H. ; Vachier, F. ; DESMARS, J. ; PEREIRA, C. L. ; SANTOS-SANZ, P. ; Sfair, R. ; DE SANTANA, T. ; ASSAFIN, M. ; VIEIRA-MARTINS, R. ; GOMES-JÚNIOR, A. R. ; MARGOTI, G. ; DHILLON,

V. S. ; FERNÁNDEZ-VALENZUELA, E. ; BROUGHTON, J. ; BRADSHAW, J. ; BENEDETTI-ROSSI, G. ; et.al . A dense ring of the trans-Neptunian object Quaoar outside its Roche limit. Nature, v. 614, p. 239-243, 2023.

- Rommel et al. 2023: ROMMEL, F. L. ; Braga-Ribas, F. ; Ortiz, J. L. ; SICARDY, B. ; SANTOS-SANZ, P. ; DESMARS, J. ; CAMARGO, J. I. B. ; VIEIRA-MARTINS, R. ; ASSAFIN, M. ; MORGADO, B. E. ; BOUFLEUR, R. C. ; BENEDETTI-ROSSI, G. ; GOMES-JÚNIOR, A. R. ; FERNÁNDEZ-VALENZUELA, E. ; HOLLER, B. J. ; SOUAMI, D. ; Duffard, R. ; MARGOTI, G. ; VARA-LUBIANO, M. ; Lecacheux, J. ; et.al . A large topographic feature on the surface of the trans-Neptunian object (307261) 2002 MS 4 measured from stellar occultations. ASTRONOMY & ASTROPHYSICS, v. 678, p. A167, 2023.

- Morgado et al. 2024: MORGADO, B. E. ; SICARDY, B. ; Braga-Ribas, F. ; Ortiz, J. L. ; SALO, H. ; VACHIER, F. ; DESMARS, J. ; PEREIRA, C. L. ; SANTOS-SANZ, P. ; Sfair, R. ; DE SANTANA, T. ; ASSAFIN, M. ; VIEIRA-MARTINS, R. ; GOMES-JÚNIOR, A. R. ; MARGOTI, G. ; DHILLON, V. S. ; FERNÁNDEZ-VALENZUELA, E. ; Broughton, J. ; BRADSHAW, J. ; BENEDETTI-ROSSI, G. ; et.al . Author Correction: A dense ring of the trans-Neptunian object Quaoar outside its Roche limit. Nature, v. 626, p. E2-E2, 2024.

- Pereira et al. 2024: PEREIRA, C L ; BRAGA-RIBAS, F ; SICARDY, B ; GOMES-JÚNIOR, A R ; ORTIZ, J L ; BRANCO, H C ; CAMARGO, J I B ; MORGADO, B E ; VIEIRA-MARTINS, R ; ASSAFIN, M ; BENEDETTI-ROSSI, G ; DESMARS, J ; EMILIO, M ; MORALES, R ; ROMMEL, F L ; HAYAMIZU, T ; GONDOU, T ; JEHIN, E ; ARTOLA, R A ; ASAI, A ; et.al . Physical properties of Centaur (60558) 174P/Echeclus from stellar occultations. MONTHLY NOTICES OF THE ROYAL ASTRONOMICAL SOCIETY, v. 527, p. 3624-3638, 2023.

- Sicardy et al. 2024: SICARDY, B. ; TEJ, A. ; GOMES-JÚNIOR, A. R. ; ROMANOV, F. D. ; BERTRAND, T. ; ASHOK, N. M. ; LELLOUCH, E. ; MORGADO, B. E. ; ASSAFIN, M. ; DESMARS, J. ; CAMARGO, J. I. B. ; KILIC, Y. ; Ortiz, J. L. ; VIEIRA-MARTINS, R. ; Braga-Ribas, F. ; NINAN, J. P. ; BHATT, B. C. ; PRAMOD KUMAR, S. ; SWAIN, V. ; BENEDETTI-ROSSI, G. ; et.al . Constraints on the evolution of the Triton atmosphere from occultations: 1989-2022. ASTRONOMY & ASTROPHYSICS, v. 682, p. L24, 2024.

- Rizos et al. 2024: RIZOS, J. L. ; FERNÁNDEZ-VALENZUELA, E. ; Ortiz, J. L. ; ROMMEL, F. L. ; SICARDY, B. ; MORALES, N. ; SANTOS-SANZ, P. ; Leiva, R. ; VARA-LUBIANO, M. ; MORALES, R. ; KRETLOW, M. ; ALVAREZ-CANDAL, A. ; HOLLER, B. J. ; Duffard, R. ; GÓMEZ-LIMÓN, J. M. ; DESMARS, J. ; SOUAMI, D. ; ASSAFIN, M. ; BENEDETTI-ROSSI, G. ; Braga-Ribas, F. ; et.al . A study of centaur (54598) Bienor from multiple stellar occultations and rotational light curves. ASTRONOMY & ASTROPHYSICS, v. 689, p. A82, 2024.

- Kretlow et al. 2024: KRETLOW, M. ; Ortiz, J. L. ; DESMARS, J. ; MORALES, N. ; ROMMEL, F. L. ; SANTOS-SANZ, P. ; VARA-LUBIANO, M. ; FERNÁNDEZ-VALENZUELA, E. ; ALVAREZ-CANDAL, A. ; Duffard, R. ; Braga-Ribas, F. ; SICARDY, B. ; CASTRO-TIRADO, A. ; FERNÁNDEZ-GARCÍA, E. J. ; SÁNCHEZ, M. ; SOTA, A. ; ASSAFIN, M. ; BENEDETTI-ROSSI, G. ; BOUFLEUR, R. ; CAMARGO, J. I. B. ; et.al . Physical properties of trans-Neptunian object (143707) 2003 UY 117 derived from stellar occultation and photometric observations. ASTRONOMY & ASTROPHYSICS, v. 691, p. A31, 2024.

4.8 Considerações Finais

O projeto foi realizado conforme o planejado, considerando algumas pequenas modificações necessárias para adaptação às novas publicações e resultados publicados. O estudo da captura dos satélites irregulares é uma consequência natural dos próximos passos deste trabalho, que está em andamento.

Participei de diversos eventos de divulgação e disciplinas para o ensino de astronomia, ajudando na melhoria e reconhecimento do departamento e na formação de novos alunos e profissionais.

A colaboração nacional e internacional foi fundamental para estender os meios de atuação, ajudar colaboradores do departamento a participar destas colaborações e me inserir em outras novas.

Portanto, acredito que o projeto tenha sido de grande valia para a instituição e mostra o comprometimento e a importância do trabalho realizado, além de abrir possibilidades de projetos futuros.

A Artigo publicado na revista MNRAS

Monthly Notices of the ROYAL ASTRONOMICAL SOCIETY

MNRAS **526,** 4435–4454 (2023) https://doi.org/10.1093/mnras/stad3017
Advance Access publication 2023 October 5

Accretion of ice giant planets from massive protoplanets whose migration is blocked by Jupiter and Saturn

G. Benedetti-Rossi ,[1,2★] R. Ribeiro,[1★] O. C. Winter,[1] H. S. Gaspar[3] and E. Vieira-Neto[1]

[1]*Universidade Estadual Paulista Julio de Mesquita Filho, Grupo de Dinâmica Orbital e Planetologia, Av. Dr. Ariberto Pereira da Cunha, 333 - Pedregulho, Guaratinguetá - SP, 12516-410, Brazil*
[2]*Laboratório Interinstitucional de e-astronomia, LIneA/MCTI & INCT do e-Universo, Rio de Janeiro, Brazil*
[3]*Universidade Federal de Santa Catarina, Estr. Dona Francisca, 8300 - Bloco U - Zona Industrial Norte, Joinville - SC, 89219-600, Brazil*

Accepted 2023 October 2. Received 2023 September 29; in original form 2023 May 15

ABSTRACT

The growth and dynamical evolution of protoplanets beyond Saturn through collisions and type I migration typically result in a highly chaotic dynamics, producing a diversity of outcomes depending on the initial conditions. Here we present the results of N-bodies numerical simulations aiming to make a detailed exploration of different initial conditions and potential outcomes for this dynamics. We consider Jupiter and Saturn at the imminence of crossing the 3:2 mean motion resonance in two possible positions based on the final and initial conditions of the Grand Tack and the Nice models, respectively; four different gas disc lifetimes, and a range of population sizes of planetary embryos beyond Saturn with different masses and orbital configurations in a total of 72 different setups. We present statistical analyses of our outcomes including planets that 'jump' to interior orbits of Jupiter, the frequency of close encounters between the planetary embryos and Jupiter, the number of ejections and collisions, and the dynamical effects for stabilizing the final planetary system in chains of mean motion resonances. Results show that independently of the initial configuration of Jupiter and Saturn and the gas lifetime, the dynamical evolution goes through three main phases. A few per cent of the simulations successfully produce Uranus and Neptune analogues, which may have implications on the ice giants' composition and obliquities, the material ejected from the Solar System, and the conditions for the giant planet instability.

Key words: planets and satellites: dynamical evolution and stability – planets and satellites: formation.

1 INTRODUCTION

In our Solar System, Uranus and Neptune are also called ice giant planets because during their formation they incorporated material as either ice or gas trapped in water-ice (Hofstadter et al. 2011; Molaverdikhani, Henning & Mollière 2019a, b). The complete process for their formation and evolution can be explained in general terms, but it is yet to be fully explained. Within the environment of dust and gas, the planetary formation scenario is very complex, being divided in a few phases, according to the dominant processes involved in the growth scales in the protoplanetary disc (Blum & Wurm 2000; Rodmann et al. 2006; Johansen & Lambrechts 2017). Early studies showed that the growth of the ice giants by planetesimal accretion takes longer than the gas disc lifetime (Safronov 1969; Levison & Stewart 2001; Thommes & Lissauer 2003). This phenomenon occurs even when the distance from the Sun is at 10–15 au, as noted in Levison, Thommes & Duncan (2010).

Pebble accretion, i.e. the growth by the capture of mm-cm sized objects that aerodynamically drift through the disc, has been shown to drastically accelerate core growth throughout the gas disc (Lambrechts & Johansen 2012, 2014). Depending on the initial fluxes of pebbles in the disc, cores of ice giant planets with a mass of 10–20 Earth masses ($M_{\oplus}$) can form within the lifetime of the gas disc, as shown by Lambrechts, Johansen & Morbidelli (2014), even when accounting for gravitational interactions among the growing protoplanets (Levison, Kretke & Duncan 2015). Pebble accretion, however, is expected to produce planets with zero obliquity (Dones & Tremaine 1993; Johansen & Lacerda 2010).

The ∼3-degree obliquity of Jupiter and the ∼27-degree obliquity of Saturn can be explained by spin-orbit resonances with Uranus and Neptune, respectively (Hamilton & Ward 2004; Ward & Hamilton 2004; Boué, Laskar & Kuchynka 2009; Brasser & Lee 2015; Vokrouhlický & Nesvorný 2015). On the other hand, Uranus and Neptune's obliquities of ∼98 and ∼30 degrees, respectively, are thought to be the result of giant collisions during their formation (Slattery, Benz & Cameron 1992; Boué & Laskar 2010; Jakubík et al. 2012; Morbidelli et al. 2012; Kegerreis et al. 2018). If this is the case, Uranus and Neptune cannot have formed solely by pebble accretion.

Izidoro et al. (2015a) proposed that the ice giants formed in two steps. By the time Jupiter and Saturn had undergone rapid gas accretion to become giants, pebble accretion had produced a system of protoplanets of ∼5 Earth masses, comparable in mass to most

★ E-mail: gugabrossi@gmail.com (GB-R); r.sousa@unesp.br (RR)

© The Author(s) 2023.
Published by Oxford University Press on behalf of Royal Astronomical Society. This is an Open Access article distributed under the terms of the Creative Commons Attribution License (https://creativecommons.org/licenses/by/4.0/), which permits unrestricted reuse, distribution, and reproduction in any medium, provided the original work is properly cited.

Downloaded from https://academic.oup.com/mnras/article/526/3/4435/7291961 by guest on 24 October 2023

super-Earths (e.g. Mayor et al. 2011; Batalha et al. 2013; Marcy et al. 2014; Wolfgang, Rogers & Ford 2016). These protoplanets migrated inwards in the Type-I regime due to tidal torques from the gas disc (Goldreich & Tremaine 1980; Ward 1986; Tanaka, Takeuchi & Ward 2002). While it is unclear whether Jupiter and Saturn at this point would have been migrating inwards, outwards, or have roughly stationary orbits (Masset & Snellgrove 2001; Morbidelli & Crida 2007; Pierens & Nelson 2008; Pierens & Raymond 2011; Pierens et al. 2014; Raymond & Morbidelli 2014), the gas giants' migration was certainly slower than that of the protoplanets for typical disc viscosities. In addition, the co-presence of Jupiter and Saturn has the effect to slow down, stop, or reverse, the resonant migration of these two planets, depending on the aspect ratio of the disc (Crida & Morbidelli 2007).

The protoplanets that formed beyond the gas giants' orbits cannot generally migrate past the orbits of Jupiter and Saturn; rather, the gas giants act as a migration barrier (Izidoro, Morbidelli & Raymond 2014; Izidoro et al. 2015b). Protoplanets become trapped in mean motion resonances (MMR) with Saturn, and successive protoplanets form chains of MMRs. As more protoplanets migrate inwards, the resonant chain is destabilized, leading to giant (obliquity-generating) collisions and another phase of migration into resonant chains. According to Izidoro et al. (2015a), this process typically produces 2–3 ice giants with masses comparable to those of Uranus and Neptune in resonant chains that include Jupiter and Saturn. The work by Izidoro et al. (2015a, b) points to a good direction towards solving the ice giants' formation, where they conclude that accretion from inelastic collisions among planetary embryos is a plausible scenario for the origin of Uranus and Neptune and their obliquities.

The dynamical evolution of the protoplanets through type I migration and blocked by gas giant planets results in a highly chaotic dynamics, producing a diversity of outcomes depending on the initial conditions, which were not deeply explored in previous work. Moreover, motivated by the initial conditions of the Grand Tack model (Walsh et al. 2011), Izidoro et al. (2015a) put Jupiter and Saturn on fixed orbits at 3.5 au and 4.58 au, respectively, while Tsiganis et al. (2005) and Nesvorný & Morbidelli (2012) put the giant planets at a more spread configuration for the Nice model. Due to the high uncertainty of the natal region of gas giant planets, it is necessary to explore the formation of ice giant planets considering other initial conditions.

In this work, we aim to make a detailed exploration of different initial conditions and potential outcomes for the formation of ice giant planets after Jupiter and Saturn, using type I migration and motivated by the orbital kinematics adopted by Izidoro et al. (2015a). In our scenario, we consider Jupiter and Saturn with $a > 5$ au, in two different positions based on the final conditions of the Grand Tack model (Walsh et al. 2011) and the initial conditions of the Nice model (Tsiganis et al. 2005; Nesvorný & Morbidelli 2012), both with Jupiter and Saturn at the imminence of crossing the 3:2 MMR. We assume a population of planetary embryos formed beyond Saturn's orbit, with different number, masses, and orbital configurations for its members. We also explore two different gas disc lifetimes.

With the data generated by our simulations we then perform statistical analyses of the possible outcomes for the ice giant planets' formation after Jupiter and Saturn, including the production of planets with the masses of Uranus and Neptune, planets that cross the orbits of Jupiter and Saturn, the number of close encounters (CE) between the planetary embryos and Jupiter, and the number of ejections and collisions among the planetary embryos. We also discuss the dynamical effects responsible for stabilizing or destabilizing the final planetary system in chains of MMRs.

Section 2 covers the methods, physical processes, and equations that were implemented in our numerical simulations, and their specifics are elaborated in Section 3. In Section 4 we present our results followed by a corresponding discussion, our conclusions, and final remarks in Section 5.

2 METHODS

In this work, we used N-body simulations including the effects of the gaseous protoplanetary disc inspired on the dynamical study of the formation of Uranus and Neptune made by Izidoro et al. (2015a). Here, we consider the two giant planets fully formed with two different initial configurations: (i) a more compact system, i.e. Jupiter and Saturn are on fixed circular orbits at 5 and 6.55 au, respectively (hereafter, tight – TI), and (ii) a wide configuration (hereafter, wide – WI), consisting of Jupiter and Saturn on fixed circular orbits at 5.4 and 7.07 au, respectively. These two configurations were motivated by the mentioned final conditions of the Grand Tack model (Walsh et al. 2011) or the initial conditions of the Nice model (Tsiganis et al. 2005; Nesvorný & Morbidelli 2012). In both cases, Jupiter and Saturn are at the imminence to cross the 3:2 MMR.

We did not consider the migration of Jupiter and Saturn in our simulations. It is important to note that the actual migration history of Jupiter and Saturn is not well known. Deienno et al. (2022) show that it would be difficult to reconcile the current low mass of the main asteroid belt with the possibility that Jupiter migrated from distances beyond 15 au, while Bitsch et al. (2015), for example, using a disc evolution and pebble accretion, claimed that a giant planet ending at 5 au can only form from a seed initially located beyond 20 au.

Beyond the orbits of the gas giant planets, in each simulation we considered embedded in the gas disc a population of planetary embryos. Different numbers of embryos and the total mass of such embryos' population were tested. Simulations were run over 2, 3, 5, and 9 Myr, which may correspond to the gas lifetime (Haisch, Lada & Lada 2001; Mamajek 2009). We also adopted the surface density for the gas used by Izidoro et al. (2015a) to compute the migration and tidal damping rates on the planetary embryos (see Section 2.1). The surface density of the disc accounts for the gaps opened by Jupiter and Saturn as well the partial depletion of the inner disc; this profile had been calculated using hydrodynamical simulations and has been widely tested and used in similar studies (Cresswell & Nelson 2006, 2008; Morbidelli et al. 2008; Pierens, Cossou & Raymond 2013).

We consider that Jupiter and Saturn are already fully formed and the disc has evolved sufficiently to behave as an isothermal disc. Thus, the gas temperature can be described by a simple power law ($T \propto r^{-\beta}$, with r being the heliocentric distance and β the temperature profile index; Hayashi 1981). It is important to mention that type-I migration direction is very sensitive to the disc properties (temperature, density, and viscosity) and the mass of the planetary embryos. Thus, depending on the combination of different torques acting on each planetary embryo, these objects may either migrate inwards or outwards (Ward 1986, 1997; Paardekooper & Mellema 2006; Baruteau & Masset 2008; Kley & Crida 2008; Paardekooper & Mellema 2008; Paardekooper & Papaloizou 2008; Kley, Bitsch & Klahr 2009; Lyra, Paardekooper & Mac Low 2010; Paardekooper et al. 2010; Paardekooper, Baruteau & Kley 2011; Horn et al. 2012; Kley & Nelson 2012; Bitsch et al. 2013; Cossou, Raymond & Pierens 2013; Pierens et al. 2013; Baruteau et al. 2014; Bitsch et al. 2014, 2015; Ogihara, Morbidelli & Guillot 2015; Suzuki et al. 2016). We also include in our simulations the orbital eccentricity and inclination damping due to the gravitational interaction with the gas. We focus here on a phase before the full dissipation of the gas disc, during the

Downloaded from https://academic.oup.com/mnras/article/526/3/4435/7291961 by guest on 24 October 2023

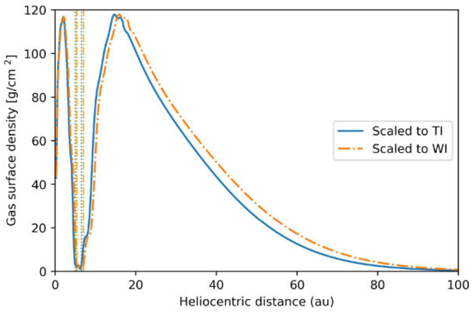

Figure 1. Surface gas density profile generated from a hydrodynamical simulation considering a minimum mass solar nebula and Jupiter and Saturn on fixed orbits – originally at 5.16 au -, and re-scaled to our two initial conditions with Jupiter at 5 au (in blue, solid line, scaled to the TI configuration) and at 5.4 au (in orange, scaled to WI). The vertical dotted and dashed lines represent the initial positions of Jupiter and Saturn in the two configurations.

formation of the ice giant planets. After the formation of the ice giant planets in our Solar System, the system may pass by a giant planet instability triggered by themselves, or by the gas dispersion, or even by the planetesimal disc (Gomes et al. 2005; Tsiganis et al. 2005; de Sousa et al. 2020; Liu, Raymond & Jacobson 2022).

2.1 Gaseous disc

The surface gas density and the velocity of the gas are interpolated from hydrodynamical simulations and performed in one dimension (Morbidelli & Crida 2007; Bitsch et al. 2015). In those simulations, Jupiter and Saturn were kept on non-migrating orbits and allowed to open a gap in the disc until an equilibrium gas distribution was achieved (Masset & Snellgrove 2001). Fig. 1 presents the fiducial gas profile based on the model of Walsh et al. (2011) in which Jupiter's positions are re-scaled so that the gap matches its initial position in our simulations, i.e. at 5.0 au for the TI setup and 5.4 au for the WI.

Close to the star the period of each planet or embryo is smaller and, as a consequence, the dynamical evolution of these objects is more influenced by the gas disc. In this work, re-scaling the gas profile to our TI and WI setups, the dynamical evolution of the planets and planetary embryos are different from Izidoro et al. (2015a) due to different orbital velocities, and consequently different migration velocities.

The gas disc dissipation in our simulations is due to viscous accretion and photoevaporation, and it was mimicked by an exponential decay of the surface density as given in equation (1):

$$\mathrm{GDF} = \exp\left(-\frac{t}{\tau_{\mathrm{gas}}}\right), \tag{1}$$

where GDF is the dissipation factor, t is the current time in the simulation, and τ_{gas} is the gas dissipation time-scale, which we considered to be 2, 3, 5, and 9 Myr. The gas disc aspect ratio (h) is given by

$$h = \frac{H}{r} = 0.033r^{0.25}, \tag{2}$$

where r is the heliocentric distance and H is the disc scale height. The disc viscous stress (ν) was modelled using the standard 'alpha' prescription for the disc viscosity $\nu = \alpha c_s H$, with $\alpha = 0.002$ (Shakura & Sunyaev 1973) and c_s is the isothermal sound speed.

2.2 Type-I migration

In our simulations, the planetary embryos feel the effects of type I migration. These planetary embryos have a few Earth masses, and they are able to launch spiral waves in the protoplanetary disc. The backreaction of these waves produces torques to the objects' orbit, therefore, causes the Type-I migration (Goldreich & Tremaine 1980; Ward 1986; Tanaka et al. 2002; Tanaka & Ward 2004). We include these effects following the prescriptions of Paardekooper et al. (2010, 2011) to build by the isothermal approximation of the gas disc. Normalized and unsaturated torques are represented by simple functions of the surface gas density and temperature gradients. Given our disc temperature profile, the temperature gradient is assumed as $\beta = 0.5$, and the local (at the location of the object) gas surface density gradient is given by

$$x = -\frac{\partial \ln \Sigma_{\mathrm{gas}}}{\partial \ln r}. \tag{3}$$

To implement the total torque experienced by the embryos in the locally isothermal limit, we followed Cresswell & Nelson (2008) and Coleman & Nelson (2014). This total torque is given by

$$\Gamma_{\mathrm{tot}} = \Gamma_L \Delta_L + \Gamma_C \Delta_C, \tag{4}$$

where Γ_L and Γ_C represent the Lindblad torque and the co-orbital contribution, respectively. Δ_L and Δ_C are the rescaling functions accounting for the reduction of the Lindblad and co-orbital torques due to the planet eccentricity and orbital inclination (Bitsch & Kley 2010, 2011; Fendyke & Nelson 2014). The function for Γ_L and the reduction factor Δ_L are defined respectively in equation (14) from Paardekooper et al. (2010) considering the factor b/h $= 0.4$, and in equation (4) from Izidoro et al. 2015a). They are presented here in equations (5) and (6) with the mentioned considerations.

$$\Gamma_L = (-2.5 - 1.7\beta + 0.1x)\Gamma_0, \tag{5}$$

$$\Delta_L = \left[P_e + \frac{P_e}{|P_e|} \times \left\{0.07\left(\frac{i}{h}\right) + 0.085\left(\frac{i}{h}\right)^4 - 0.08\left(\frac{e}{h}\right)\left(\frac{i}{h}\right)^2\right\}\right]^{-1}. \tag{6}$$

Note in equation (5) a slightly difference from equation (9) in Izidoro et al. (2015a), where they consider a factor 1.5 multiplying β instead of 1.7 used here and in Paardekooper et al. (2010). The co-orbital torque Γ_C, and the reduction factor Δ_C, are defined in Izidoro et al. (2015a) – see equations (8) and (6), respectively. They are presented here in equations (7) and (8).

$$\Gamma_C = (F(\rho_v)G(\rho_v))\Gamma_{\mathrm{hs,baro}} \\ +(1 - K(\rho_v))(\Gamma_{C,\mathrm{lin,baro}} + \Gamma_{C,\mathrm{lin,ent}}), \tag{7}$$

$$\Delta_C = \left[1 - \tanh\left(\frac{i}{h}\right)\right]\exp\left(-\frac{e}{e_f}\right), \tag{8}$$

where e_f is given by $e_f = 0.5h + 0.01$. It is important to state that there is a factor -1 in equation (8) compared to equation (6) from Izidoro et al. (2015a). The value for Γ_0 is calculated at the location of the planetary embryo and related to the planet–star mass ratio (q), the disc aspect ratio (h), the local surface density Σ_{gas}, and the planet's Keplerian frequency Ω_k, and is given by

$$\Gamma_0 = \left(\frac{q}{h}\right)^2 \Sigma_{\mathrm{gas}} r^4 \Omega_k^2. \tag{9}$$

Also, e is the planet eccentricity, i is the planet orbital inclination, and P_e is given by (from equation 13 in Cresswell & Nelson 2008)

$$P_e = \left[1 + \left(\frac{e}{2.25h}\right)^{1.2} + \left(\frac{e}{2.84h}\right)^6\right]\left[1 - \left(\frac{e}{2.02h}\right)^4\right]^{-1}. \tag{10}$$

Downloaded from https://academic.oup.com/mnras/article/526/3/4435/7291961 by guest on 24 October 2023

The co-orbital torque is expressed as the sum of the barotropic part of the horseshoed drag ($\Gamma_{\text{hs, baro}}$), the barotropic part of the linear co-rotation torque ($\Gamma_{C,\text{ lin, baro}}$), and the entropy-related part of the linear co-rotation torque ($\Gamma_{C,\text{ lin, ent}}$), given, respectively (equations 10, 11, and 12 in Izidoro et al. 2015a) by

$$\Gamma_{\text{hs,baro}} = 1.1\left(\frac{3}{2} - x\right)\Gamma_0, \tag{11}$$

$$\Gamma_{C,\text{lin,baro}} = 0.7\left(\frac{3}{2} - x\right)\Gamma_0, \tag{12}$$

$$\Gamma_{C,\text{lin,ent}} = 0.8\beta\,\Gamma_0. \tag{13}$$

Note that some equations presented in Izidoro et al. (2015a) may contain typos that were corrected here. The functions $F(p)$, $G(p)$, and $K(p)$ are given in Paardekooper et al. (2011) (equations 23, 30, and 31 respectively):

$$F(p) = \frac{1}{1 + \left(\frac{p}{1.3}\right)^2}, \tag{14}$$

$$G(p) = \begin{cases} \frac{16}{25}\left(\frac{45\pi}{8}\right)^{\frac{3}{4}} p^{\frac{3}{2}}, & p < \sqrt{\frac{8}{45\pi}} \\ 1 - \frac{9}{25}\left(\frac{8}{45\pi}\right)^{\frac{4}{3}} p^{-\frac{8}{3}}, & p \geq \sqrt{\frac{8}{45\pi}} \end{cases} \tag{15}$$

$$K(p) = \begin{cases} \frac{16}{25}\left(\frac{45\pi}{28}\right)^{\frac{3}{4}} p^{\frac{3}{2}}, & p < \sqrt{\frac{28}{45\pi}} \\ 1 - \frac{9}{25}\left(\frac{28}{45\pi}\right)^{\frac{4}{3}} p^{-\frac{8}{3}}, & p \geq \sqrt{\frac{28}{45\pi}} \end{cases} \tag{16}$$

The parameter governing saturation at the location of the planetary embryo, p_ν, is given by (equation 13 from Izidoro et al. 2015a):

$$p_\nu = \frac{2}{3}\sqrt{\frac{r^2\Omega_k}{2\pi\nu}x_s^3} \tag{17}$$

with $x_s = 1.1\sqrt{q/h}$ being the non-dimensional half-width of the horseshoe region. Finally, the time-scales for eccentricity (t_e) and inclination (t_i) damping relates to the solar mass ($\text{M}_\odot$), the embryo semimajor axis (a), mass (m), orbital inclination (i), and eccentricity (e), and they are given, respectively (equations 11 and 12 from Cresswell & Nelson 2008) by

$$t_e = \frac{t_{\text{wave}}}{0.780}\left(1 - 0.14\left(\frac{e}{h}\right)^2 + 0.06\left(\frac{e}{h}\right)^3 + 0.18\left(\frac{e}{h}\right)\left(\frac{i}{h}\right)^2\right) \tag{18}$$

$$t_i = \frac{t_{\text{wave}}}{0.544}\left(1 - 0.3\left(\frac{i}{h}\right)^2 + 0.24\left(\frac{i}{h}\right)^3 + 0.14\left(\frac{i}{h}\right)\left(\frac{e}{h}\right)^2\right) \tag{19}$$

where

$$t_{\text{wave}} = \frac{\text{M}_\odot^2 h^4}{m_p a^2 \Sigma_{\text{gas}}\Omega_k}. \tag{20}$$

We included in the equations of motion of the planetary embryos the synthetic accelerations defined in Cresswell & Nelson (2008) (equations 14, 15 and 16, respectively) to model the Type-I migration and damping of e, and i over the corresponding time-scales defined above, these accelerations are given by

$$\vec{a}_m = -\frac{\vec{v}}{t_m} \tag{21}$$

$$\vec{a}_e = -2\frac{(\vec{v}\cdot\vec{r})\,\vec{r}}{r^2 t_e}, \tag{22}$$

$$\vec{a}_i = -\frac{v_z}{t_i}\hat{k} \tag{23}$$

with $\vec{k}$ being the unit vector in the z-direction.

Table 1. Initial conditions for our simulations with the number of planetary embryos and masses.

Sim. Tag	Initial N. of embryos	Total disc mass ($M_\oplus$)	Individual embryo mass ($M_\oplus$)
2–30	2	30	15
3–45	3	45	15
5–30	5	30	6
5–50	5	50	10
5–60	5	60	12
10–50	10	50	5
10–60	10	60	6
15–60	15	60	4
20–60	20	60	3

3 NUMERICAL SIMULATIONS

We used the REBOUND code (Rein & Liu 2012; Rein & Spiegel 2015; Rein & Tamayo 2015) to perform N-body simulations of the planetary embryos interacting with the Sun, Jupiter, Saturn, and the gas of the protoplanetary disc. The simulations were performed using a hybrid MERCURIUS integrator (Rein et al. 2019) using an initial time-step of 0.5 yr.

We include in our code synthetic accelerations which mimic the Type I migration and eccentricity and inclination damping for the planetary embryos, as presented in previous sections. Physical collisions were considered to be inelastic, resulting in merging events that conserve the system's linear momentum. Planetary embryos were removed from our simulations if they reached heliocentric distances smaller than 1 au or greater than 100 au, or if eccentricities become larger than 1.

We prepared 72 different simulation setups. They were obtained by combining different initial total masses of the disc (30, 45, 50, or 60 $M_\oplus$) equally divided between the number of embryos and initial numbers of planetary embryos (2, 3, 5, 10, 15, or 20). We chose those values for the total disc mass and number of embryos in order to investigate the formation of protoplanets that could reach similar masses of Uranus and Neptune.

Table 1 presents nine simulation tags defining each configuration used, considering different initial numbers of embryos, total disc mass, and individual embryo masses. In each of those nine tags, Jupiter and Saturn were positioned respectively in circular orbits at (i) 5.0 and 6.55 au, corresponding to a more compact system (TI), and (ii) 5.4 and 7.076 au, corresponding to a more sparse system (WI).

We used an orbital control for Jupiter and Saturn that mimics the effects of Type II migration (Cresswell & Nelson 2008). Here, we have all planetary embryos also interact with the two giant planets, while Jupiter and Saturn suffer only small changes in their orbits due to the low individual masses of each embryo, as they are trapped in quasi-circular and co-planar orbits in the type II migration.

The planetary embryos were initially positioned using the following procedure: we first calculated Saturn's Hill radius and added to it the embryo Hill radius calculated at Saturn's heliocentric distance multiplied by a random factor between 5 and 10. The following embryos were positioned following the same procedure, first calculating the embryo Hill radius at its random position and adding the Hill radius multiplied by another random factor between 5 and 10. This is important because the formation of the planetary embryos by pebble accretion typically creates a gravitational stable separation between their neighbours by a factor of 5 Hill radius (Kokubo & Ida 2000).

Downloaded from https://academic.oup.com/mnras/article/526/3/4435/7291961 by guest on 24 October 2023

All initial inclinations and eccentricities of the planetary embryos were set to 0.001 degrees and 0.01, respectively, and the other orbital parameters were set randomly. Finally, to complete the 72 setups, simulations were run over a total time of 2, 3, 5, and 9 Myr, corresponding to the gas lifetime. Those values for the gas lifetime were chosen in order to study a more complete set of gas disc lifetimes. The simulations with 5 and 9 Myr could be longer than the gas disc lifetime if we consider the time for the giant planets to grow and migrate. So, typically 2 and 3 Myr could be more appropriate since there would be many exponential time-scales before the complete disc dissipation. For each of the 18 setups over 5 Myr, we performed 1000 simulations run, while 100 simulations were run over 2, 3, and 9 Myr, in a total of 23 400 simulations. We note that after 5 Myr, the system becomes stable, often locked in chains of MMRs, with very few close interactions (see Section 4.1 for details). Therefore, the majority of interactions happen in the first 2 and 3 Myr. Based on this, we performed simulations with 2, 3, and 9 Myr for the gas lifetime in a smaller number. As also noticed in Izidoro et al. (2015a), 2 and 3 Myr may not be enough time for the system, if a large number of initial planetary embryos is considered, to reach a final stable configuration, where the embryos end up in resonant chains. So, we focus and performed a high number of simulations considering 5 Myr (also a good case for the gas disc phase lifetime).

4 RESULTS

In this section, we present the results from the 23 400 numerical simulations with the 72 different initial setups described in Section 3. The typical features of the evolution of planetary embryos are shown in Section 4.1. We then present a comparison between the two initial setups for Jupiter and Saturn, the TI and WI configurations – Section 4.2. Later, we present some interesting characteristics such as the number of embryos ejections and merges, the CE with Jupiter, and the presence of embryos in the inner solar system in Sections 4.3, 4.4, and 4.5, respectively. Finally, we study the formation of Uranus and Neptune analogues in Section 4.6 and present the results for the good cases only in Section 4.7.

4.1 Evolution of the planets and planetary embryos

Fig. 2 shows the periapsis (q), semimajor axis (a), and apoapsis (Q) evolution of planets and planetary embryos for four different setups. Panels (a), (c), and (e) show the TI configuration for a gas lifetime of 2, 5, and 9 Myr, respectively. Panels (b), (d), and (f) show the WI configuration for a gas lifetime of 3, 5, and 9 Myr, respectively. Panels (c) and (d) are simulations starting with 15 embryos, while the others start with 20 planetary embryos each. We note that in all cases, the highest number of close interactions (e.g. close encounters) among the giant planets and planetary embryos occur within the first ∼1.5 Myr, independently of the gas disc lifetime. Rare mergers, ejections, or strong interactions occur between these objects after 4 Myr. In general, we noticed only a few differences in simulations with different gas lifetimes or setups (TI versus WI). A typical feature in our simulations is the high number of close encounters between the planetary embryos and the giant planets (∼2000 CE per simulation). We also found that some planetary embryos can jump the orbits of the giant planets and be implanted in the inner Solar System (hereafter named jumpers) or can be placed in a 1:1 MMR and survive as co-orbitals. At the end of the gas disc phase, it is typical to find only 2 or 3 planetary embryos left, even in the simulations with high initial number of planetary embryos.

For the cases where the gas disc has a smaller lifetime (2 and 3 Myr) and an initial number of planetary embryos larger than 10, the planetary embryos often are not locked in final chains of MMRs at the end of the gas disc phase (see also in Izidoro et al. 2015a). The planetary embryos that are locked in final chains of mean motion at the end of the gas disc phase are called here as possible stable configurations. de Sousa et al. (2020) showed that about 50–60 per cent of these possible stable configurations are actually not stable after the gas disc phase. Specifically, we found that 2 per cent to 5 per cent of the simulations starting with 2, 3, and 5 planetary embryos are not in possible stable configurations at the end of the gas disc phase in all setups, whereas this number increases to 50 per cent to 96 per cent if we start the simulation with 20 embryos considering 2 or 3 Myr, respectively. Therefore, there is not enough time for the system to reach a final possible stable configuration where the embryos end up in resonant chains considering smaller gas lifetime, as can be clearly noted in Fig. 2. It is worth mentioning that what happens with these planetary systems after the gas dissipation is out of the scope of this paper.

The dynamical evolution of the planets and planetary embryos can be summarized in three main stages. The first stage occurs when most of the strong and closest interactions between the planets and planetary embryos occur. During this stage, the planetary embryos' eccentricities reach very high values due to close encounters. The trigger for the first stage is the type-I migration of the planetary embryos, which places them in closer orbits towards the orbits of Jupiter and Saturn relatively fast. This stage happens until 1.5 Myr and varies depending on the initial mass of the planetary embryos and the gas disc density. The first stage is always unstable and is a set for planetary instabilities (close encounters, collisions, and ejections of planets).

The second stage typically happens between ∼1.5 and ∼4 Myr when the remaining planetary embryos are captured in MMRs between them and Jupiter and Saturn, reaching equilibrium eccentricities usually ≤0.1. There is a very small number of closest interactions between these bodies at this second stage. Note that for the simulations with the gas lifetime of 2 and 3 Myr there is not enough time for the planetary embryos to be captured, reach the eccentricities equilibrium, and continue the next stage. The third stage happens after ∼4 Myr, where the system is stabilized and continues until the end of the integration, with very rare number of simulations presenting instabilities in only 4 per cent of the simulations. The fraction of the simulations which present instabilities at the third stage is only approximately 6 per cent in the simulations where the gas lifetime was considered to be 9 Myr. As can be seen in Fig. 2 panels (a) and (c) compared to panels (c) and (d), we found that increasing the lifetime of the gas to 9 Myr does not change the global picture of the dynamical evolution of the planets and planetary embryos.

4.2 Gas giant planets in different initial positions

We used in our simulations two main different sets of initial conditions for Jupiter and Saturn, named TI and WI, as explained in Section 2. The giant planets were initially positioned close to the 3:2 MMR. We did not perform any simulation assuming that giant planets start in the 2:1 MMR. Our methodology involves hydrodynamical simulations related to the properties of the protoplanetary disc. Therefore, we are only considering an isothermal disc with a total mass compatible with the minimum-mass solar nebula, following Pierens et al. (2014), which leads to a typical capturing of the 3:2 MMR between Jupiter and Saturn. For discussion purposes, we

Downloaded from https://academic.oup.com/mnras/article/526/3/4435/7291961 by guest on 24 October 2023

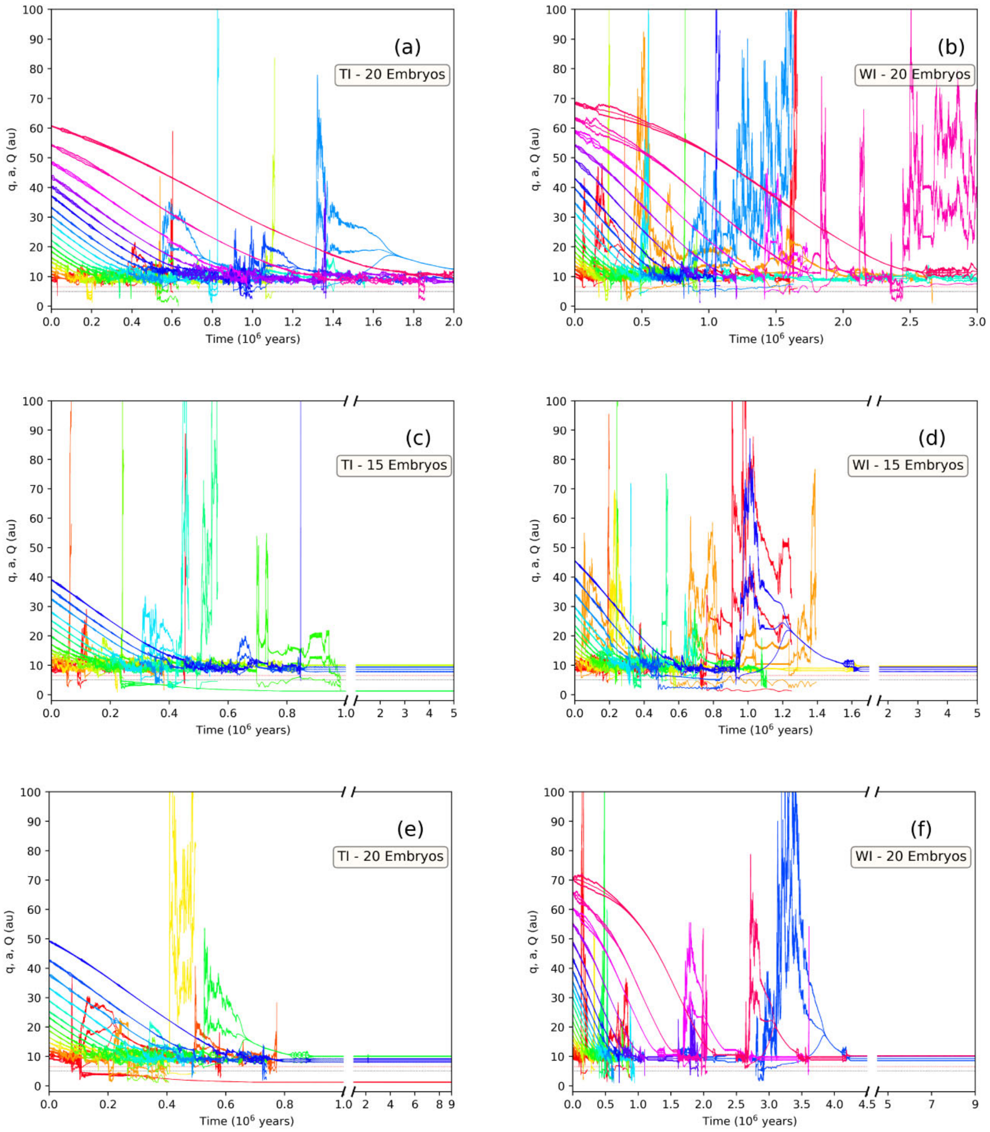

Figure 2. Six simulations starting with total disc mass of 60 $M_{\odot}$ selected to illustrate the evolution of their periapsis (q), semimajor axis (a), and apoapsis (Q) versus time. Panels (a), (c), and (e) show the TI configuration for a gas lifetime of 2, 5, and 9 Myr, respectively. Panels (b), (d), and (f) show the WI configuration for a gas lifetime of 3, 5, and 9 Myr, respectively. Panels (c) and (d) are simulations starting with 15 embryos, while the others start with 20 planetary embryos each. Different colours represent each embryo q, a, and Q, while dashed lines are the positions for Jupiter (black) and Saturn (red).

believe that the 2:1 MMR is a very strong resonance and could produce different final MMR chains or lead to more instability phases during the dynamical evolution of the planetary embryos. However, we also think that the gas disc properties and the high masses of Jupiter and Saturn are the most important factors influencing these effects. In general, our results show that there are no significant differences between the two configuration adopted.

Note in Fig. 2 that the dynamical evolution of the embryos are very similar with only a small delay for a second series of close interactions between the embryos, which happens around 0.8 Myr for the TI configuration while it is after 1 Myr for the WI.

Concerning the interactions between the planetary embryos and other characteristics, presented in detail in the next sections, the fraction of merges and the ejection of at least half of the initial number

Downloaded from https://academic.oup.com/mnras/article/526/3/4435/7291961 by guest on 24 October 2023

Table 2. Correlation factors between close encounters with Jupiter and ejection instant.

Gas lifetime (Myr)	TI r	TI p-factor	WI r	WI p-factor
2	0.876	1.4×10^{-13}	0.856	2.0×10^{-12}
3	0.859	1.6×10^{-18}	0.845	2.1×10^{-17}
5	0.782	8.4×10^{-22}	0.795	5.1×10^{-23}
9	0.777	1.2×10^{-37}	0.808	1.8×10^{-40}

Table 3. Simulation fraction (per cent) where one or more embryos finished the simulations in the inner solar system (1 au < a < 5 au).

Tag	Simulations TI	WI
2–30	0.0	0.0
3–45	0.0	0.0
5–30	1.2	0.7
5–50	0.0	0.0
5–60	0.0	0.0
10–50	2.3	2.9
10–60	2.4	2.5
15–60	4.5	3.7
20–60	8.6	8.3

of embryos are respectively 1–5 per cent and 1–9 per cent more likely to happen in the TI setups (values are presented in Tables A1, A4, and A5 in the Appendix). The number of close encounters, the presence of jumpers, and the formation of Uranus and Neptune good analogues (UN-analogues) are very similar between the setups and do not show preference for one of the configuration (values are presented in Tables A6, A7, in the Appendix, and Table 3).

4.3 Merges and ejections

In Fig. 3, we present the occurrence frequency of mergers among planetary embryos, defined as the ratio of simulations resulting in merges (including those with no mergers) to the total number of simulations performed for each setup. It is worth noting that simulations starting with two embryos cannot result in more than one merge, as well as simulations starting with three embryos cannot result in more than two merges.

The frequency of 0 merges is greater than 87 per cent for cases with an initial number of 2 and a total solid disc mass of 30 Earth masses. In this scenario, where there are initially only two planetary embryos, the system is often stable during the second stage (see Section 4.1). If we do not consider the simulations starting with two embryos, the frequency of one merge ranges from 21–44 per cent. Conversely, the frequency of four or more merges is rare (less than 7 per cent) at any stage. The frequency of two and three merges falls between 5–28 per cent and 1–10 per cent, respectively. Furthermore, the number of merges increases with the initial number of planetary embryos, and only one or two merges are produced in about 45–65 per cent of our simulations starting with five or more embryos.

The number of merges of the TI setup is slightly bigger (1–5 per cent) than the WI setup, in general. The planetary embryos usually start in a more compact configuration when Jupiter and Saturn are in TI setup, increasing the chance of the closest encounters among the planetary embryos, and consequently the number of merges.

Fig. 4 presents the occurrence frequency of simulations in which it was ejected 0 to 20 planetary embryos in our different setups. The number of ejections increases with the initial number of planetary embryos, having simulations starting with 20 objects always presenting more than 10 ejections. Note that the occurrence frequencies of ejections for the TI setups are 1–9 per cent more likely to eject at least 50 per cent of the planetary embryos than the WI setups although, in general, they are very similar if we directly compare ejections of a specific number of planetary embryos. The occurrence frequency of ejections also does not change too much when increasing the gas lifetime. It is important to note that for simulations considering the gas lifetime of 2 and 3 Myr the system did not reach the equilibrium in MMR chains and some embryos may be ejected later. Additionally, nearly all planetary embryos are ejected in about 50–65 per cent of the simulations, regardless of the number of initial embryos, remaining 1 to 3 planetary embryos until the end of integration. For example, note in the simulations starting with 10 embryos and total disc mass of 50 Earth masses that 6 to 8 planetary embryos are ejected in approximately 75 per cent of the simulations. It is important to point out that the total mass of the remaining embryos may vary, since merged planetary embryos may be ejected or remain until the end of the simulations.

4.4 Close encounters with Jupiter

We detected the number of close encounters (CE) between the planetary embryos and Jupiter. An event of CE is detected when the planetary embryo gets inside three mutual Hill radius. We track the orbital evolution during the close encounter when they reach one mutual Hill radius.

Fig. 5 shows the number of CE between Jupiter and a planetary embryo in all our simulations. Most of the CE happens in the first half million years, regardless of the initial setup, with approximately 2000 CE per simulation. Note that there is a small fraction (∼2 per cent) of CE events that occur later than the first stage. We refer to this occurrence as the second peak of close encounters. We have observed that this is a typical phenomenon in simulations with a small number of initial planetary embryos with approximately 50 per cent of the CE happening at this time for simulations starting with 2 embryos, 5–10 per cent for simulations starting with 3 or 5 embryos, and less than 1 per cent of CE happening in this second peak for simulations with higher number of embryos. As previously described, planetary embryos can be quickly captured in chains of MMRs. For example, when there are only two initial planetary embryos, the chains of MMRs are usually 3:2–6:5 MMR or 3:2–7:6 MMR. In these configurations, the planetary embryos are closer to each other, and as the gas density decreases over time, the eccentricity of their orbits grows, and close interactions between the planetary embryos typically occur, producing a late instability. This late instability results in the second peak of close encounters between the planetary embryos and Jupiter. For the simulations starting with a higher number of embryos, those MMR chains are rapidly broken, or they do not even happen due to the outer embryos' interaction causing instability in the system during all the period where the gas has the most influence.

It is also important to highlight that the time-scale of close encounters with Jupiter, presented in Fig. 5, correlates directly with the ejection instant. In fact, Table 2 presents the Pearson's rank correlation (Press et al. 1996) for all the setups. All factors were calculated using a bin of 50 thousand years and the very small p-factor indicates a very strong correlation.

Downloaded from https://academic.oup.com/mnras/article/526/3/4435/7291961 by guest on 24 October 2023

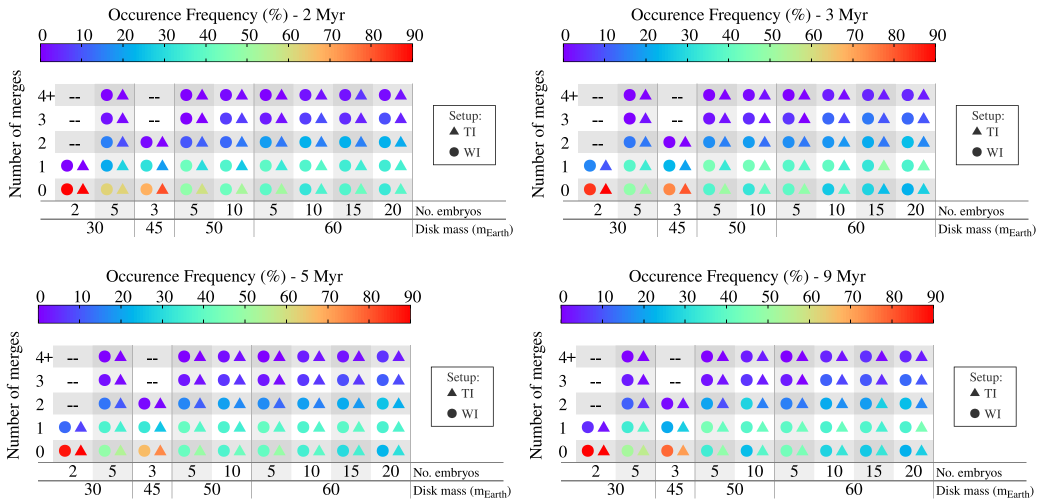

Figure 3. Number of merges between embryos and the occurrence frequency in simulations. Lines present the simulations in which 0, 1, 2, 3, and 4 or more embryos merged while columns represent the different setups with the initial number of embryos and total disc mass, while circles and triangles represent different setups (WI and TI, respectively). Top panel are the simulations considering the gas lifetime of 2 and 3 Myr while the bottom panel presents the simulations for 5 and 9 Myr.

4.5 Jumpers

In some of our simulations, one or more planetary embryos may typically cross the orbit of Jupiter, ending in the inner part of the solar system with a semimajor axis between 1 and 5 au, as presented in Table 3. Those 'jumpers' also appear in simulations made by Izidoro et al. (2015a, b) and Jakubík et al. (2012) and seem to be a direct consequence of the interaction with gas surface density assumed for the protoplanetary discs. Ribeiro de Sousa et al. (2022) showed that some protoplanets, which are being scattered by Jupiter, enter the inner region of the Solar System for a short period of time and can affect the capture process of planetesimals (for example, Ceres-sized objects) in the inner region of the Solar System. They referred to these protoplanets as 'invaders,' and our simulations indicate that these objects are common.

4.6 Good analogues of Uranus and Neptune

We consider the Uranus and Neptune good analogues (UN-analogues) the planetary embryos within the mass range between 11.09 and 20.59 Earth masses, which correspond approximately to the average mass of the two ice giants ± 30 per cent of this value.

Fig. 6 presents the occurrence frequency of 1 to 3 UN-analogues in our simulations. It is important to highlight that the total number of simulations that ended with two or three planetary embryos is 40–70 per cent of our simulations in all setups, regardless of the number of initial planetary embryos. Note also that for simulations starting with 2, 3, or 60 Earth masses and 5 planetary embryos, the individual embryo masses already satisfy this range, while for the other simulations starting with 5 or more planetary embryos, it is necessary that at least two merges in order to have a UN-analogue.

For simulations starting with two embryos, we consider as a good case the simulations where both planetary embryos survived until the end of the simulations, i.e. there are no ejections or merges. This represents 30–43 per cent of the simulations with the gas lifetime 3, 5, and 9 Myr, while it is around 75–82 per cent for the two setups considering the gas lifetime of 2 Myr (see Table 4). Note that with a smaller gas lifetime, the gas dispersion is very fast, making it difficult a substantial migration of the planetary embryos and the close interaction with the other bodies, so it is expected a higher fraction of simulations ending with 2 in these cases. We note that in the good cases the planetary embryos start initially distributed between 8 and 13 au, usually the innermost planetary embryo finish between this same range, concentrating in semimajor axis values near to the 9:4 MMR with Jupiter and 3:2 MMR with Saturn. The outermost planetary embryos usually finish between 9.8 and 10.6 au in the TI setups, and between 10.3 and 11.5 au, respectively, close to seven main MMRs: the 3:1 MMR with Jupiter, the 2:1 MMR with Saturn, and the 7:6, 6:5, 5:4, or 4:3 MMR with the innermost planetary embryo. Those results are independent of the gas lifetime used in our simulations (2, 3, 5, or 9 Myr).

Simulations starting with three planetary embryos we consider as a good case the ones that finish with two or three planetary embryos, which are 56–69 per cent of the simulations with the gas lifetime 3, 5, and 9 Myr, while it is 84–87 per cent for the two setups considering 2 Myr. Simulations finishing with three planetary embryos represent 6–12 per cent of the total. Note here that in there may have happened one ejection or merge, but in the later case the planetary embryo is no longer considered as a UN-analogue as it reaches 30 Earth masses, which is outside our range. In 27–43 per cent of the simulations, one planetary embryo was ejected, and they finish with two planetary embryos having the same mass (and considered UN-analogues). This number is higher for the 2 Myr setups, with 48 per cent and 57 per cent in the TI and WI configuration, respectively. Considering the cases where one merge happened, in 12–18 per cent of the simulations the inner planetary embryo is bigger than the outer planetary embryo, while only 1–

Downloaded from https://academic.oup.com/mnras/article/526/3/4435/7291961 by guest on 24 October 2023

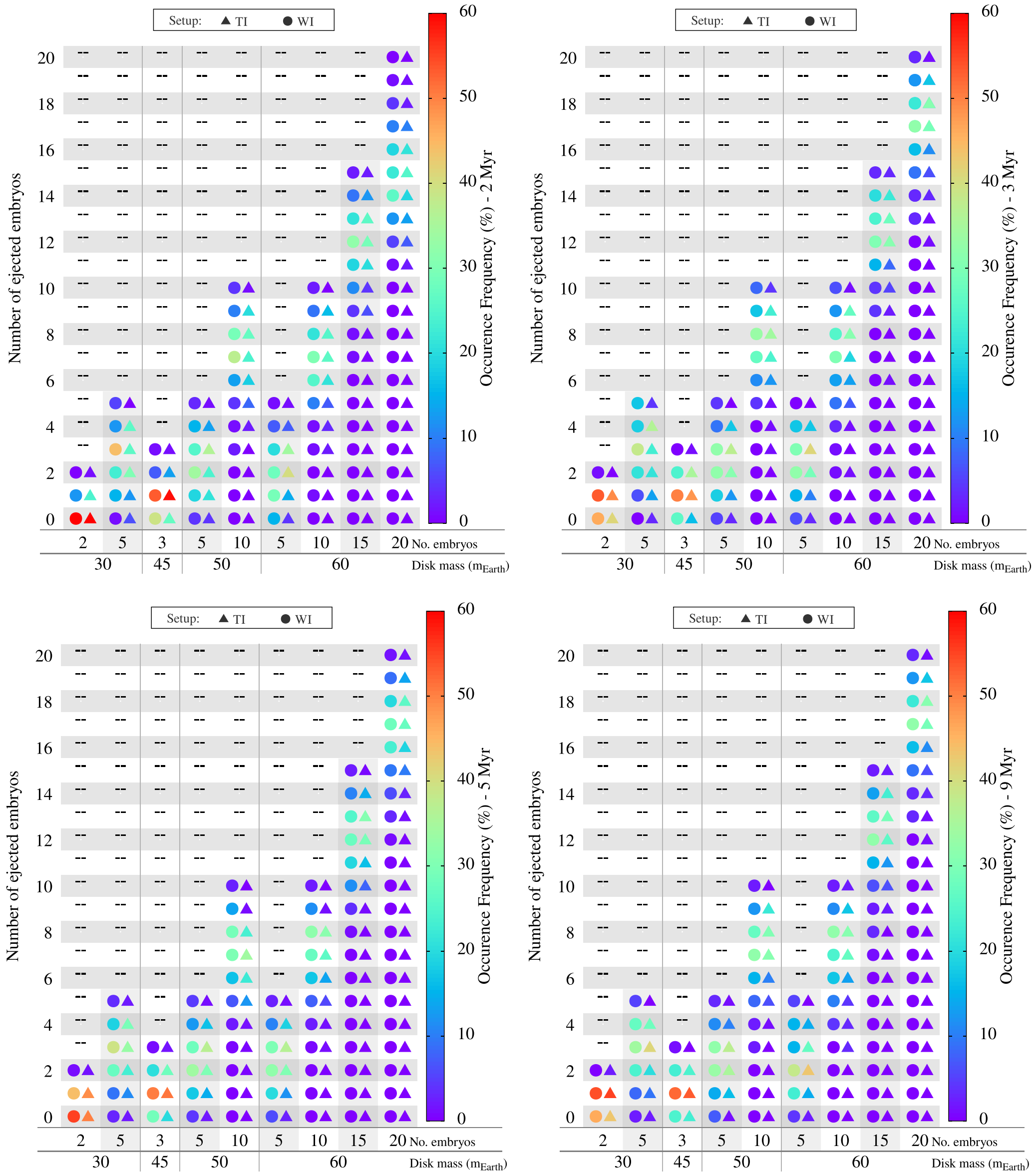

Figure 4. Occurrence frequency in simulations in which it was ejected 0 to 20 embryos. Columns represent the different setups with initial number of embryos and total disc mass, while circles and triangles represent different setups (WI and TI, respectively). The upper panels present the occurrence frequency for the simulations considering the gas lifetime of 2 and 3 Myr while the lower panels present the simulations for 5 and 9 Myr.

3 per cent of the cases the outer planetary embryo is bigger. In all those cases, similar to the case with two planetary embryos, simulations start with distributed planetary embryos between 8 and 15 au, and they finish in similar configurations, close to the same MMRs. For simulations ending with three planetary embryos, the outermost planetary embryo is usually close to the same MMRs with respect to the second planetary embryo (7:6, 6:5, 5:4, or 4:3).

The last setup in this group are simulations starting with five planetary embryos and total mass of $60M_{\oplus}$, also initially satisfying the condition of each planetary embryo to be a UN-analogue,

Downloaded from https://academic.oup.com/mnras/article/526/3/4435/7291961 by guest on 24 October 2023

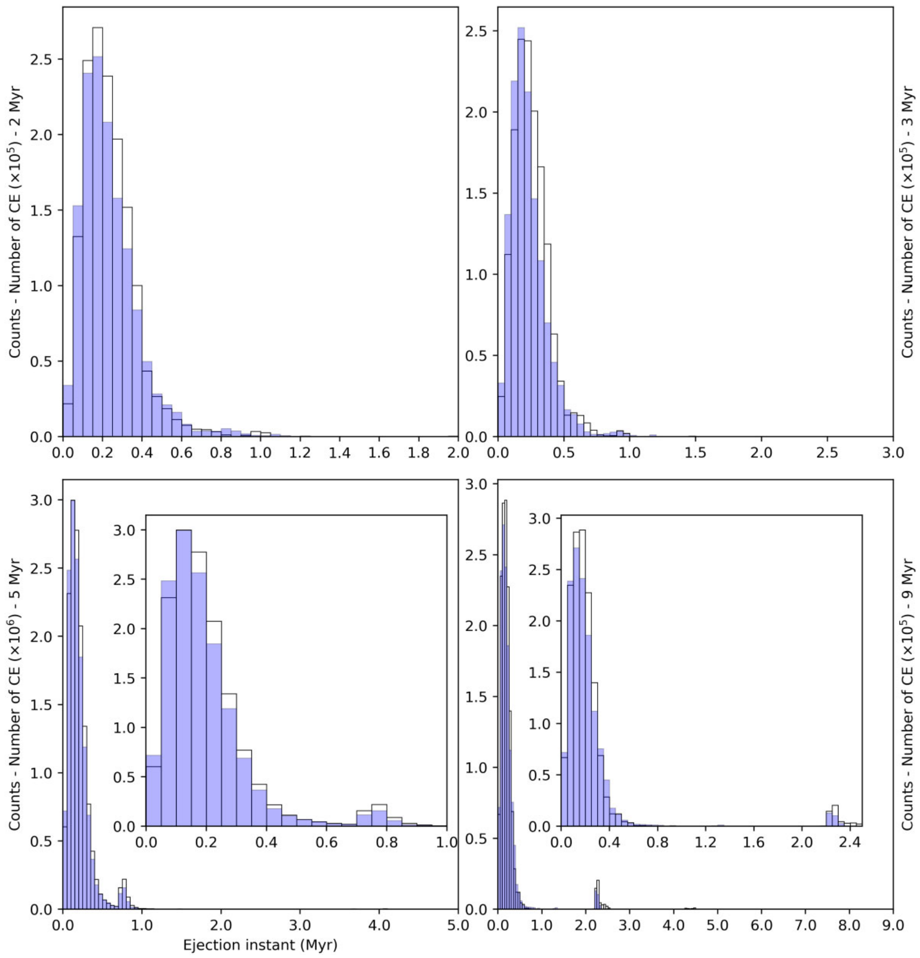

Figure 5. Histograms presenting the number of close encounter between a planetary embryo and Jupiter. Transparent boxes represent the simulations for the TI setup, while coloured boxes are for the WI. Top panels show simulations with a gas lifetime of 2 Myr (left) and 3 Myr (right), while bottom panels show simulations with a gas lifetime of 5 Myr (left) and 9 Myr (right). Inset plots on the lower panels present a zoom in the initial region when the most number of CE happened.

needing it only to survive until the end of each simulation. Here, we consider as good case the simulations that finishes with 2 or 3 planetary embryos, so a higher number of merges or ejections may have happened. The good cases here represent 59–76 per cent of the simulations in all setups. Simulations that finishes with 2 or 3 planetary embryos and no merge happened, i.e. the planetary embryos survived from the beginning and the others were ejected, represent 26–32 per cent of the simulations in the TI configuration and 38 to 54 per cent in the WI setups. We note that 11–22 per cent finished with two planetary embryos, and 5 to 11 with three planetary embryos in the TI setups, while it is 28–32 per cent, and 5–11 per cent finishing with two, and three planetary embryos in the WI setups, respectively. Simulations finishing with four planetary embryos (one planetary embryo is two times more massive than the other three) only are present in the cases where the gas lifetime is 2 or 5 Myr, and they represent only 1 per cent of those simulations. There was no case where simulations finished with five planetary embryos. Again, all simulations start with distributed planetary embryos between 8.5 and 20 au, they also finish in the same MMR configuration as the two previous cases, close to those main four resonant chains with the inner planetary embryo (7:6, 6:5, 5:4, or 4:3).

As presented in Section 4.3, the low number of merges and the high number of ejections causes a production of small number of UN-analogues, so it is expected a higher fraction of simulations which already starts with planetary embryos within this mass range to produce more UN-analogues when comparing with simulations with a higher number of planetary embryos, which consequently has lower individual masses. In fact, in 35–55 per cent of the simulations starting with planetary embryos having 6 to 15 Earth masses, they finish with at least 1 UN-analogue, while it is 0–15 per cent if

Downloaded from https://academic.oup.com/mnras/article/526/3/4435/7291961 by guest on 24 October 2023

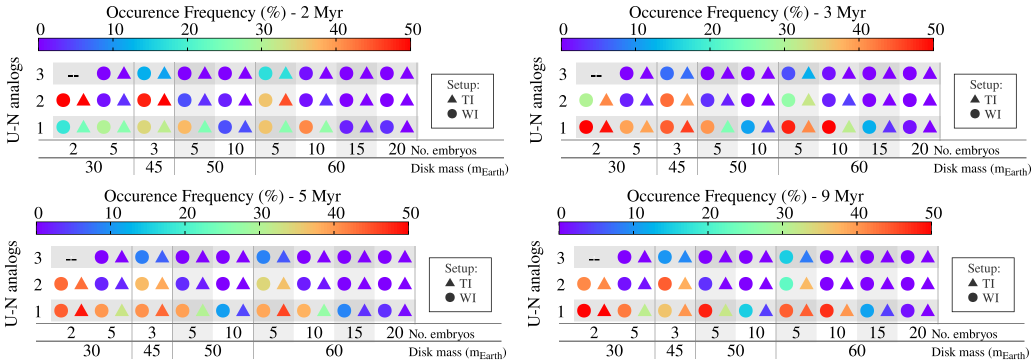

Figure 6. Simulations frequency ending with two or three planetary embryos and forming one to three UN-analogues. Columns represent the different setups with initial number of planetary embryos and total disc mass, while circles and triangles represent different setups (WI and TI, respectively). Top panel presents the occurrence frequency for the simulations considering the gas lifetime of 2 and 3 Myr, while the bottom panel presents the simulations for 5 and 9 Myr.

Table 4. Percentage of simulations considered good cases (finished with 2, or 3 UN-analogues) and the total number of planetary embryos at the end.

		Final number of planetary embryos									
Gas	Sim.	2 Embryos		3 Embryos		4 Embryos		5 + Embryos		Total (per cent)	
Lifetime	ID	TI	WI	TI	WI	TI	WI	TI	WI	TI	WI
	2–30	82	75	–	–	–	–	–	–	82	75
	3–45	75	72	12	12	–	–	–	–	87	84
	5–60	42	52	33	24	–	–	–	–	75	76
	5–30	17	15	6	7	0	2	0	0	23	24
2 Myr	5–50	25	12	11	11	0	4	0	0	36	27
	10–60	21	13	13	9	2	0	1	0	37	22
	10–50	4	3	2	0	0	0	0	0	6	3
	15–60	2	2	0	0	0	0	0	0	2	2
	20–60	0	0	1	0	1	0	1	0	3	0
	2–30	30	41	–	–	–	–	–	–	30	41
	3–45	62	49	7	7	–	–	–	–	69	56
	5–60	51	42	10	17	–	–	–	–	61	59
	5–30	19	22	0	6	0	0	0	0	19	28
3 Myr	5–50	28	15	6	4	1	0	0	0	35	19
	10–60	25	16	5	4	0	0	0	0	30	20
	10–50	4	2	0	0	0	0	0	0	4	2
	15–60	1	0	1	1	0	0	0	0	2	1
	20–60	0	0	0	0	0	0	0	0	0	0
	2–30	43.2	42.8	–	–	–	–	–	–	43.2	42.8
	3–45	56.4	51.1	8.2	6.2	–	–	–	–	64.6	57.3
	5–60	50.0	52.6	19.2	10.1	–	–	–	–	69.2	62.7
	5–30	21.9	19.8	3.9	4.8	0.1	0.3	0.0	0.0	25.9	24.9
5 Myr	5–50	24.7	18.2	7.4	5.6	0.3	0.1	0.0	0.0	32.4	23.9
	10–60	22.8	14.2	5.6	4.0	0.8	0.7	0.0	0.1	29.2	19.0
	10–50	4.7	2.7	2.0	1.1	0.3	0.0	0.0	0.0	7.0	3.8
	15–60	3.2	1.4	2.5	0.8	0.7	0.1	0.0	0.0	6.4	2.3
	20–60	0.9	0.4	0.8	0.1	0.4	0.0	0.0	0.0	2.1	0.5
	2–30	41	41	–	–	–	–	–	–	41	41
	3–45	57	51	10	9	–	–	–	–	67	60
	5–60	40	60	26	12	–	–	–	–	69.2	62.7
	5–30	25	13	0	6	0	1	0	0	25	20
9 Myr	5–50	26	16	6	9	1	0	0	0	33	25
	10–60	32	15	1	7	0	3	0	0	33	25
	10–50	8	2	3	0	0	0	0	0	11	2
	15–60	2	0	2	1	0	0	0	0	4	1
	20–60	0	0	0	0	0	0	0	0	0	0

Downloaded from https://academic.oup.com/mnras/article/526/3/4435/7291961 by guest on 24 October 2023

Table 5. Number of simulations with the different final configuration.

Configuration	2 Myr TI	2 Myr WI	3 Myr TI	3 Myr WI	5 Myr TI	5 Myr WI	9 Myr TI	9 Myr WI	Number of UN-Analogues	Mass Ratio
Four remaining planetary embryos										
E - 3E - 2E - E	1	0	0	0	0	0	0	0	2	0.7
2E - E - 2E - E	0	0	0	0	0	1	0	0	2	1.0
2E - E - 3E - E	0	0	0	0	0	0	0	1	2	1.5
3E - 2E - E - E	0	0	0	0	0	0	0	1	2	0.7
Three remaining planetary embryos										
E - 2E - 2E	0	0	0	0	1	2	1	0	2	1.0
2E - 2E - E	1	1	0	2	17	7	3	0	2	1.0
2E - E - 2E	1	1	0	0	3	1	0	0	2	1.0
3E - 3E - E	1	0	0	0	0	1	0	0	2	1.0
3E - 2E - E	1	0	0	0	2	1	0	0	2	0.7
2E - 2E - 2E	0	0	1	0	0	0	0	0	3	1.0
2E - 3E - 3E	0	0	1	0	0	0	0	0	3	1.5
4E - 3E - 2E	0	0	0	0	1	0	0	0	3	0.5
Two remaining planetary embryos										
2E - 2E	5	5	6	8	40	36	8	1	2	1.0
3E - 3E	1	0	0	0	1	1	0	0	2	1.0
3E - 2E	0	1	2	1	6	6	2	0	2	0.7
2E - 3E	0	0	0	0	1	1	0	0	2	1.5

Note. **E** is the minimum mass in the setup, i.e. 2E means that the planetary embryo undergone through one collision and ended with two of its initial mass. The mass ratio is calculated using the mass of the outermost UN-analogue divided by the mass of the innermost one. Note that for each of the 18 setups over 5 Myr, we performed 1000 simulations run, while 100 simulations were run over 2, 3, and 9 Myr, in a total of 23 400 simulations.

planetary embryos start with lower masses. Furthermore, in 22–41 per cent of the simulations with planetary embryos starting within the UN-analogue mass range it was formed 2 UN-analogues, while it is less than 3 per cent for the other simulations. If we consider the presence of three UN-analogues in the end of our simulations, it happens only in less than 10 per cent of the simulations starting with planetary embryos within the mass range.

Considering the final position of the planetary embryos, in < 10 per cent of the simulations made by Izidoro et al. (2015a) they produce UN-analogues where the second innermost planetary embryo (beyond Saturn) is larger than the innermost one. Our results show that, in general, very few simulations finishes with the outermost planetary embryo being larger than the innermost one. If we exclude simulations starting with two or three embryos (which already start in the UN-analogue mass range), we find that nearly 1–4 per cent of the simulations produce a more massive planetary embryo in the outer part. For simulations starting with 2 or 3 planetary embryos, approximately 35–44 per cent of them remained with two UN-analogues of the same size at the end of integration, while around 10 per cent of the simulations starting with three planetary embryos finished with the outermost planetary embryo larger than the innermost one (see Table A8).

4.7 The good cases for the solar system

The subset of simulations where it was formed two UN-analogues beyond the orbit of Saturn, experienced at least one collision each, and their mass ratio is $0.7 \leq M1/M2 \leq 1.5$, deserve a special attention because they may present some interesting connections to other studies in the Solar System. In this section, we play special attention to those cases (good cases hereafter).

As mentioned in previous section, some of our simulations already start with the embryos satisfying the criteria to be a UN-analogue, so they may not experience a collision event, and they just need to survive until the end of the integration (simulation tags 2–30, 3–45, and 5–60). Due to this fact, we only consider here the simulations with other setups (the ones with tags 5–30, 5–50, 10–50, 10–60, 15–60, and 20–60). Interestingly, 99 per cent of the simulations in those setups end only with two or three planetary embryos, as presented in Table 4. However, four cases starting with 10 embryos and 60M$_\odot$ finished with four embryos where two of them are UN-analogues.

It is important to highlight that for each of the setups we used, there may be needed a different number of collision events in order for the planetary embryo to become a UN-analog. Simulations with tag 5–50 need only one collision, while for the simulations with tags 5–30 and 10–60, one or two events may happen and the planetary embryo will be in the mass range. The simulations with tags 10–50, 15–60, and 20–60 can form UN-analogues if the planetary embryos experience 2 or 3; 2, 3, or 4; and 3, 4, or 5 collisions, respectively.

Table 5 present the number of simulations with good cases for the solar system with their final configuration and mass ratio. Note that in most of the good cases – 156 in total – both planetary embryos finish with the same mass (mass ratio 1.0) meaning that they have undergone through two or three collisions each to be formed. In only four cases the outermost embryo finishes with bigger mass compared to the innermost one, while in 25 cases the innermost is smaller. In total, the number of good cases represent close to 1 per cent of our simulations.

The initial position of the planetary embryos does not seem to play an important role in the final configuration. The first planetary embryo is positioned after 8 au in all the good cases, and the last planetary embryo is at approximately 20, 35, 55, and 77 au for simulations starting with 5, 10, 15, and 20 planetary embryos. However, in all the good cases the planetary embryos finish between 8 and 20 au, always positioned close to the MMRs chains as the first

Downloaded from https://academic.oup.com/mnras/article/526/3/4435/7291961 by guest on 24 October 2023

Table 6. Possible chains of MMRs for the system with Jupiter, Saturn, and the remaining planetary embryos in our good analogues of Uranus and Neptune.

Simulations that ended with two good analogues of Uranus and Neptune
(3:2, 3:2, 7:6)
(3:2, 3:2, 6:5)
(3:2, 3:2, 5:4)
(3:2, 3:2, 4:3)
Simulations that ended with three good analogues of Uranus and Neptune
(3:2, 3:2, 7:6: 7:6 or 6:5 or 4:3 or 5:4)
(3:2, 3:2, 6:5, 7:6 or 6:5 or 4:3 or 5:4)
(3:2, 3:2, 5:4, 7:6 or 6:5 or 4:3 or 5:4)
(3:2, 3:2, 4:3, 7:6 or 6:5 or 4:3 or 5:4)

group. We did not find any preferable resonant chain, i.e. there is no rule for the planetary embryo to reach the final position, and they may finish in any of the mentioned MMRs. We may also conclude here that a higher number of planetary embryos may cause very unstable systems which causes more ejections, making it difficult for the formation of UN-analogues.

The summary of the chains of mean motions found in our simulations of good analogues of Uranus and Neptune can be found in Table 6. Simulations that ended with 2 and 3 good analogues of Uranus and Neptune in particular chains of MMRs (3:2, 3:2, 4:3), (3:2, 3:2, 4:3, 4:3), and (3:2, 3:2, 4:3, 5:4) are compatible with what was found in Morbidelli & Crida (2007) and were selected by Nesvorný & Morbidelli (2012) to study the evolution after the gas disc dissipation in the Nice model. Nesvorný & Morbidelli (2012) concluded that they are promising for producing the final orbital structure of the outer Solar System, especially for systems with five planets with mass similar to Uranus/Neptune and placed on an orbit exterior to Saturn's in a 4:3 MMR and a planetesimal disc with a total mass of 35 Earth masses. Our study points out many other possible MMRs that produce good analogues of Uranus and Neptune, which were not studied in Nesvorný & Morbidelli (2012).

5 DISCUSSION AND CONCLUSIONS

In this paper we simulate the evolution of planetary embryos with a few Earth masses during the gas phase for 2, 3, 5, and 9 Myr in order to study the interaction between those objects, the close encounters with the giant planets, and the formation of UN-analogues for a comparison with the solar system.

We prepared 72 different setups to run 23 400 simulations using two different initial positions for Jupiter and Saturn, being in a more compact (TI) or more distant (WI) configuration. For those two configurations we randomly positioned, within 5–10 mutual Hill radius, different number of planetary embryos (2,3,5,10, 15, and 20) with different initial total mass of the disc (30, 45, 50, and 60 Earth masses).

Our simulations can be divided in three main phases, the first being when most of the close interactions between the planetary embryos and the giant planets happens, the second when the system stabilizes in MMRs between the remaining planetary embryos, and the third where just a few close interactions happens. The results from our simulations show that there are no substantial differences between the different setups, although they present some particularities. When we compare the gas lifetimes of 2, 3, 5, and 9 Myr there is only one small difference at the time of the second peak presented in the histogram in Fig. 5. This second peak happens in simulations with initial low number of planetary embryos (2, 3, or 5) and are related to the dispersion of the gas and the instability of a chain of MMRs between the embryos.

Comparing the initial conditions for the positions of Jupiter and Saturn, the TI and WI setups, our results suggest that the outcome of the simulations is not strongly dependent on the initial conditions for Jupiter and Saturn and that the dynamics of the planetary embryos are mainly determined by the gravitational interactions among themselves, with Jupiter, and the gas disc. However, we cannot rule out the possibility that more subtle differences in the initial conditions, such as Jupiter and Saturn not being in circular orbits, could have a significant impact on the final outcome, and further investigations are needed to fully explore this possibility.

Exploring the planetary embryos' interaction, we first note the presence of a small fraction of simulation with objects that ended in the inner planetary system (with semimajor axis between 1 and 5 au). Those 'jumpers' also appeared in the simulations made by Izidoro et al. (2015a, b) with an occurrence upper limit of less than 20 per cent for simulations starting with a disc mass of $30M_\oplus$ to $\sim$40 per cent for simulations with a disc mass starting with $60M_\oplus$, and Jakubík et al. (2012) with even higher fraction. Although those values are higher than the values we obtained in our simulations, as presented in Table 3, the jump rate difference and estimates can be explained for several reasons. First, Jakubík et al. (2012) assumed a higher gas surface density and it remains constant during their integration.

For the comparison with results from Izidoro et al. (2015a), it is not clear if the authors consider all the planetary embryos that entered this innermost region or just the ones that survived until the end of the simulations, as it is our case. Also, we assumed a cutoff value for the semimajor axis assumed here to be 1 au while Izidoro et al. (2015a) assumed to be 0.1 au. Besides that, the jump rate is overestimated in both cases due to the assumption of isothermal type-I migration for planetary embryos and no type-II migration for the gas giants. This overestimates the differential migration between the two populations. Lastly, we assumed equal-mass planetary embryos, which produce stronger instabilities than for planetary embryos with unequal masses (Raymond, Armitage & Gorelick 2010).

Analysing the growth of the planetary embryos in our simulations, our results indicate that nearly half of the initial mass is ejected from the system (see Fig. 4) and consequently it decreases the probability of merges (see Fig. 3) and the formation of embryos with higher masses than the ones initially positioned. This has also consequences in the formation of UN-analogues, which results that Uranus and Neptune must have been formed with a similar initial mass other than formed though collisions between smaller planetary embryos. This result indicates that there is a lot of mass-loss from the initial disc of planetary embryos and that the formation of UN-analogues (representing the two ice giants) has a very low probability to happen through merges of the planetary embryos, meaning that it is more likely that Uranus and Neptune were already formed with a similar mass to the actual value, as can be seen in fig. 6, however our simulations can be biased because most of the initial planetary embryos' mass start with of those of the ice giants planets. Our best results in terms of forming two UN-analogues were obtained in simulations that start with planetary cores with masses equal to $15M_\oplus$ (two or three embryos) or $12M_\oplus$ (five embryos).

Looking into the subset of simulations which formed good UN-analogues, our result shows that the largest subset of good cases for the solar system are the ones where the simulations already started with planetary embryos with similar masses to Uranus and Neptune. A second group of good cases are the ones starting

Downloaded from https://academic.oup.com/mnras/article/526/3/4435/7291961 by guest on 24 October 2023

with five or 10 embryos and individual masses of 6 to 10 $M_{\odot}$. Neglecting the cases where the embryo just need to survive and selecting the simulations that formed two or three UN-analogues that experienced at least one collision each and their mass ratio is close to 1, the number of total good cases drop to approximately 1 per cent. None the less, there are no noticeable differences in the final configuration for the MMRs chains comparing the good cases with the others. Simulations starting with a large number of planetary embryos produce very few good cases, but further investigation is needed considering higher initial masses. However, this may have implications on the total mass of the disc.

We also study the statistics of close encounters between embryos and Jupiter. This is important to better understand their interactions and possible capture (and survival) of moons (Nesvorný, Vokrouhlický & Deienno 2014) which is out of the scope of this paper. During the first phase (until ~1.5 Myr), most of the close interactions happens between the embryos and with the giant planets with around 2000 CE with Jupiter per simulation. Despite the large amount of close encounters, only a small fraction of embryos is scattered into the inner solar system, which is consistent with the structure of our solar system. Also, a 'second wave' of CE happens after a few hundred thousand years in the simulations with a low number of initial planetary embryos. This late instability happens because when a low number of planetary embryos are quickly captured in chains of MMRs (usually 3:2–6:5 MMR or 3:2–7:6 MMR) they get closer to each other, and as the gas density decreases over time, the eccentricity of their orbits grows, occurring close interactions between the planetary embryos with a consequently late instability. This late instability is rare in simulations starting with a higher number of embryos, because those MMR chains are rapidly broken, or they do not even happen due to the outer embryos' interaction causing instability in the system during all the period where the gas has the most influence.

To conclude, explaining the formation of Uranus and Neptune and their obliquities remains uncertain. In addition, although pointing to a good direction, further analysis is still needed considering different initial conditions and other physical aspects for positioning Jupiter and Saturn.

ACKNOWLEDGEMENTS

This work was possible thanks to the scholarship granted from the Brazilian Federal Agency for Support and Evaluation of Graduate Education (CAPES), in the scope of the Program CAPES-PrInt, process number 88887.310463/2018-00, Mobility number 88887.571156/2020-00. RR thanks to the scholarship granted from the Brazilian Federal Agency for Support and Evaluation of Graduate Education (CAPES), in the scope of the Program CAPES-PrInt (Proc 88887.310463/2018-00, Mobility number 88887.572647/2020-00, 88887.468205/2019-00). This research was supported in part by the São Paulo Research Foundation (FAPESP) through the computational resources provided by the Center for Scientific Computing (NCC/GridUNESP) of the São Paulo State University (UNESP). RR also acknowledges the support provided by grants FAPESP (Proc 2016/24561-0) and by Sao Paulo State University (PROPe 13/2022).

DATA AVAILABILITY

The data underlying this article will be shared on reasonable request to the corresponding author.

REFERENCES

Baruteau C., Masset F., 2008, ApJ, 678, 483
Baruteau C. et al., 2014, in Beuther H., Klessen R. S., Dullemond C. P., Henning T., eds, Protostars and Planets VI. Lunar and Planetary Institute, Houston, TX, p. 667
Batalha N. M. et al., 2013, ApJS, 204, 24
Bitsch B., Kley W., 2010, A&A, 523, A30
Bitsch B., Kley W., 2011, A&A, 530, A41
Bitsch B., Crida A., Morbidelli A., Kley W., Dobbs-Dixon I., 2013, A&A, 549, A124
Bitsch B., Morbidelli A., Lega E., Crida A., 2014, A&A, 564, A135
Bitsch B., Johansen A., Lambrechts M., Morbidelli A., 2015, A&A, 575, A28
Blum J., Wurm G., 2000, Icarus, 143, 138
Boué G., Laskar J., 2010, ApJ, 712, L44
Boué G., Laskar J., Kuchynka P., 2009, ApJ, 702, L19
Brasser R., Lee M. H., 2015, AJ, 150, 157
Coleman G. A. L., Nelson R. P., 2014, MNRAS, 445, 479
Cossou C., Raymond S. N., Pierens A., 2013, A&A, 553, L2
Cresswell P., Nelson R. P., 2006, A&A, 450, 833
Cresswell P., Nelson R. P., 2008, A&A, 482, 677
Crida A., Morbidelli A., 2007, MNRAS, 377, 1324
de Sousa R. R., Morbidelli A., Raymond S. N., Izidoro A., Gomes R., Vieira Neto E., 2020, Icarus, 339, 113605
Deienno R., Izidoro A., Morbidelli A., Nesvorný D., Bottke W. F., 2022, ApJ, 936, L24
Dones L., Tremaine S., 1993, Icarus, 103, 67
Fendyke S. M., Nelson R. P., 2014, MNRAS, 437, 96
Goldreich P., Tremaine S., 1980, ApJ, 241, 425
Gomes R., Levison H. F., Tsiganis K., Morbidelli A., 2005, Nature, 435, 466
Haisch K. E., Jr, Lada E. A., Lada C. J., 2001, ApJ, 553, L153
Hamilton D. P., Ward W. R., 2004, AJ, 128, 2510
Hayashi C., 1981, Prog. Theor. Phys. Suppl., 70, 35
Hofstadter M., Butler B., Gurwell M., Sandell G., Atreya S., Mihalka K., 2011, EPSC-DPS Joint Meeting 2011, 691
Horn B., Lyra W., Mac Low M.-M., Sándor Z., 2012, ApJ, 750, 34
Izidoro A., Morbidelli A., Raymond S. N., 2014, ApJ, 794, 11
Izidoro A., Morbidelli A., Raymond S. N., Hersant F., Pierens A., 2015a, A&A, 582, A99
Izidoro A., Raymond S. N., Morbidelli A., Hersant F., Pierens A., 2015b, ApJ, 800, L22
Jakubík M., Morbidelli A., Neslušan L., Brasser R., 2012, A&A, 540, A71
Johansen A., Lacerda P., 2010, MNRAS, 404, 475
Johansen A., Lambrechts M., 2017, Annu. Rev. Earth Planet. Sci., 45, 359
Kegerreis J. A. et al., 2018, ApJ, 861, 52
Kley W., Crida A., 2008, A&A, 487, L9
Kley W., Nelson R. P., 2012, ARA&A, 50, 211
Kley W., Bitsch B., Klahr H., 2009, A&A, 506, 971
Kokubo E., Ida S., 2000, Icarus, 143, 15
Lambrechts M., Johansen A., 2012, A&A, 544, A32
Lambrechts M., Johansen A., 2014, A&A, 572, A107
Lambrechts M., Johansen A., Morbidelli A., 2014, A&A, 572, A35
Levison H. F., Stewart G. R., 2001, Icarus, 153, 224
Levison H. F., Thommes E., Duncan M. J., 2010, AJ, 139, 1297
Levison H. F., Kretke K. A., Duncan M. J., 2015, Nature, 524, 322
Liu B., Raymond S. N., Jacobson S. A., 2022, Nature, 604, 643
Lyra W., Paardekooper S.-J., Mac Low M.-M., 2010, ApJ, 715, L68
Mamajek E. E., 2009, in Usuda T., Tamura M., Ishii M., eds, AIP Conf. Proc. Vol. 1158, Exoplanets and Discs: Their Formation and Diversity. Am. Inst. Phys., New York, p. 3
Marcy G. W. et al., 2014, ApJS, 210, 20
Masset F., Snellgrove M., 2001, MNRAS, 320, L55
Mayor M. et al., 2011, preprint (arXiv:1109.2497)
Molaverdikhani K., Henning T., Mollière P., 2019a, ApJ, 873, 32
Molaverdikhani K., Henning T., Mollière P., 2019b, ApJ, 883, 194
Morbidelli A., Crida A., 2007, Icarus, 191, 158

Downloaded from https://academic.oup.com/mnras/article/526/3/4435/7291961 by guest on 24 October 2023

Morbidelli A., Crida A., Masset F., Nelson R. P., 2008, A&A, 478, 929
Morbidelli A., Tsiganis K., Batygin K., Crida A., Gomes R., 2012, Icarus, 219, 737
Nesvorný D., Morbidelli A., 2012, AJ, 144, 117
Nesvorný D., Vokrouhlický D., Deienno R., 2014, ApJ, 784, 22
Ogihara M., Morbidelli A., Guillot T., 2015, A&A, 584, L1
Paardekooper S. J., Mellema G., 2006, A&A, 459, L17
Paardekooper S. J., Mellema G., 2008, A&A, 478, 245
Paardekooper S. J., Papaloizou J. C. B., 2008, A&A, 485, 877
Paardekooper S. J., Baruteau C., Crida A., Kley W., 2010, MNRAS, 401, 1950
Paardekooper S. J., Baruteau C., Kley W., 2011, MNRAS, 410, 293
Pierens A., Nelson R. P., 2008, A&A, 482, 333
Pierens A., Raymond S. N., 2011, A&A, 533, A131
Pierens A., Cossou C., Raymond S. N., 2013, A&A, 558, A105
Pierens A., Raymond S. N., Nesvorny D., Morbidelli A., 2014, ApJ, 795, L11
Press W. H., Teukolsky S. a., Vetterling W. T., Flannery B. P., 1996, Numerical Recipes in Fortran 77: the Art of Scientific Computing, Vol. 1. 2nd edn., Cambridge Univ. Press, Cambridge
Raymond S. N., Morbidelli A., 2014, in Knezevic Z., Lemaitre A., eds, Proc. IAU Symp. 310, Complex Planetary Systems. Cambridge Univ. Press, Cambridge, p. 194
Raymond S. N., Armitage P. J., Gorelick N., 2010, ApJ, 711, 772
Rein H., Liu S. F., 2012, A&A, 537, A128
Rein H., Spiegel D. S., 2015, MNRAS, 446, 1424
Rein H., Tamayo D., 2015, MNRAS, 452, 376
Rein H. et al., 2019, MNRAS, 485, 5490
Ribeiro de Sousa R., Morbidelli A., Gomes R., Neto E. V., Izidoro A., Alves A. A., 2022, Icarus, 379, 114933
Rodmann J., Henning T., Chandler C. J., Mundy L. G., Wilner D. J., 2006, A&A, 446, 211
Safronov V. S., 1969, Evoliutsiia doplanetnogo oblaka. Nauka, Moscow
Shakura N. I., Sunyaev R. A., 1973, A&A, 24, 337
Slattery W. L., Benz W., Cameron A. G. W., 1992, Icarus, 99, 167
Suzuki T. K., Ogihara M., Morbidelli A., Crida A., Guillot T., 2016, A&A, 596, A74
Tanaka H., Ward W. R., 2004, ApJ, 602, 388
Tanaka H., Takeuchi T., Ward W. R., 2002, ApJ, 565, 1257
Thommes E. W., Lissauer J. J., 2003, ApJ, 597, 566
Tsiganis K., Gomes R., Morbidelli A., Levison H. F., 2005, Nature, 435, 459
Vokrouhlický D., Nesvorný D., 2015, ApJ, 806, 143
Walsh K. J., Morbidelli A., Raymond S. N., O'Brien D. P., Mandell A. M., 2011, Nature, 475, 206
Ward W. R., 1986, Icarus, 67, 164
Ward W. R., 1997, Icarus, 126, 261
Ward W. R., Hamilton D. P., 2004, AJ, 128, 2501
Wolfgang A., Rogers L. A., Ford E. B., 2016, ApJ, 825, 19

APPENDIX A: SIMULATION STATISTICS

In this section we present the tables with values used to plot Figs 3 to Fig. 6. Table A1 present values used in Fig. 3 concerning the statistics of merges while Tables A2, A3, A4, and A5 are the values for Fig. 4 with regard to embryo ejections. Data for the histograms of close encounters with Jupiter showed in Fig. 5 is presented here in Table A6. Table A7 presents values used in Fig. 6 with reference to the formation of UN-analogues. Finally, Table A8 presents the number of simulation finishing with 1, 2, or 3 UN-analogue and the total number of remaining embryos in the good cases where the outer embryo has equal mass or is larger than the others.

Downloaded from https://academic.oup.com/mnras/article/526/3/4435/7291961 by guest on 24 October 2023

Table A1. Fraction of simulations (per cent) with merges.

Gas Lifetime	Sim. ID	No merge TI	No merge WI	1 merge TI	1 merge WI	2 merges TI	2 merges WI	3 merges TI	3 merges WI	4 merges TI	4 merges WI	5 + merges TI	5 + merges WI
	2–30	100	100	0	0	–	–	–	–	–	–	–	–
	3–45	68	81	31	19	1	0	–	–	–	–	–	–
	5–30	62	62	21	28	15	9	2	1	0	0	–	–
	5–50	48	59	42	30	10	11	0	0	0	0	–	–
2 Myr	5–60	39	51	39	33	19	14	3	2	0	0	–	–
	10-50	42	52	37	26	12	14	7	7	1	1	1	0
	10-60	32	36	37	38	22	15	7	9	2	2	0	0
	15−60	37	41	34	34	22	15	5	4	2	6	0	0
	20−60	33	38	34	35	22	21	9	4	1	2	1	0
	2–30	84	90	16	10	–	–	–	–	–	–	–	–
	3–45	74	80	23	20	0	0	–	–	–	–	–	–
	5–30	48	50	38	34	14	14	0	2	0	0	–	–
	5–50	37	50	44	33	17	15	2	2	0	0	–	–
3 Myr	5–60	39	48	38	38	17	14	6	0	0	0	–	–
	10−50	32	40	43	43	19	13	5	2	1	0	0	2
	10−60	26	38	40	35	18	18	12	8	3	0	1	1
	15−60	28	24	32	49	21	14	14	10	4	0	1	3
	20−60	24	35	41	38	21	23	6	2	6	2	2	0
	2–30	87.8	92.4	12.2	7.6	–	–	–	–	–	–	–	–
	3–45	66.3	73.7	32.8	25.5	0.9	0.8	–	–	–	–	–	–
	5–30	48.4	53.7	36.3	35.0	13.6	10.2	1.7	0.9	0.0	0.0	–	–
5 Myr	5–50	41.1	49.3	40.6	37.9	15.8	10.9	2.5	1.9	0.0	0.0	–	–
	5–60	40.3	49.0	40.4	37.7	16.7	12.0	2.6	1.3	0.0	0.0	–	–
	10−50	36.6	41.8	36.3	34.4	19.5	16.4	6.0	5.8	1.3	0.9	0.3	0.7
	10−60	34.9	38.7	36.4	37.4	19.3	15.2	6.2	6.4	2.4	1.4	0.8	0.7
	15−60	29.5	34.8	38.5	38.9	21.1	18.5	8.8	6.4	1.2	1.2	0.9	0.2
	20−60	22.8	30.7	35.9	36.4	24.9	21.5	10.6	8.6	4.2	2.4	1.6	0.4
	2–30	95	98	5	2	–	–	–	–	–	–	–	–
	3–45	78	71	21	27	1	2	–	–	–	–	–	–
	5–30	52	56	34	38	11	5	3	1	0	0	–	–
	5–50	34	48	44	41	20	9	2	0	0	0	–	–
9 Myr	5–60	43	44	39	42	15	14	3	0	0	0	–	–
	10−50	24	38	38	41	28	15	6	3	3	0	1	0
	10−60	28	32	36	41	21	17	11	8	4	2	0	0
	15−60	26	32	37	35	19	27	10	5	5	1	3	0
	20−60	22	27	36	44	24	16	12	10	4	2	2	1

Note. We run 1000 simulations for each setup setting the gas lifetime of 5 Myr and 100 simulations for the setups using gas lifetime of 2, 3, and 9 Myr.

Table A2. Simulation fraction of ejections (per cent) considering the gas lifetime of 2 Myr.

	Sim. ID	Number of ejected embryos 0	1	2	3	4	5	6	7	8	9	10	11	12	13	14	15	16	17	18	19	20
	2–30	82	12	0	–	–	–	–	–	–	–	–	–	–	–	–	–	–	–	–	–	–
	3–45	39	53	7	1	–	–	–	–	–	–	–	–	–	–	–	–	–	–	–	–	–
	5–30	1	15	23	44	12	5	–	–	–	–	–	–	–	–	–	–	–	–	–	–	–
	5–50	4	19	34	25	15	3	–	–	–	–	–	–	–	–	–	–	–	–	–	–	–
TI	5–60	15	29	28	20	7	1	–	–	–	–	–	–	–	–	–	–	–	–	–	–	–
	10–50	0	0	0	2	1	4	13	37	29	10	4	–	–	–	–	–	–	–	–	–	–
	10–60	0	1	0	1	1	10	25	30	21	9	2	–	–	–	–	–	–	–	–	–	–
	15–60	0	0	0	0	0	0	0	1	1	4	11	19	32	21	9	2	–	–	–	–	–
	20–60	0	0	0	0	0	0	0	0	0	0	0	1	5	12	26	22	19	10	4	1	0
	2–30	75	24	1	–	–	–	–	–	–	–	–	–	–	–	–	–	–	–	–	–	–
	3–45	27	59	13	1	–	–	–	–	–	–	–	–	–	–	–	–	–	–	–	–	–
	5–30	6	12	30	26	26	0	–	–	–	–	–	–	–	–	–	–	–	–	–	–	–
	5–50	4	21	24	36	13	1	–	–	–	–	–	–	–	–	–	–	–	–	–	–	–
WI	5–60	4	14	40	34	7	1	–	–	–	–	–	–	–	–	–	–	–	–	–	–	–
	10–50	0	0	0	0	2	8	18	24	27	20	1	–	–	–	–	–	–	–	–	–	–
	10–60	0	0	0	2	3	7	21	26	25	16	0	–	–	–	–	–	–	–	–	–	–
	15–60	0	0	0	0	0	0	0	0	1	6	4	20	29	26	12	2	–	–	–	–	–
	20–60	0	0	0	0	0	0	0	0	0	0	0	2	7	13	19	25	21	10	2	1	0

Downloaded from https://academic.oup.com/mnras/article/526/3/4435/7291961 by guest on 24 October 2023

Table A3. Simulation fraction of ejections (per cent) considering the gas lifetime of 3 Myr.

	Sim.	Number of ejected embryos																				
	ID	0	1	2	3	4	5	6	7	8	9	10	11	12	13	14	15	16	17	18	19	20
	2–30	46	53	01	–	–	–	–	–	–	–	–	–	–	–	–	–	–	–	–	–	–
	3–45	26	50	24	0	–	–	–	–	–	–	–	–	–	–	–	–	–	–	–	–	–
	5–30	0	6	21	38	18	17	–	–	–	–	–	–	–	–	–	–	–	–	–	–	–
	5–50	5	18	32	32	9	4	–	–	–	–	–	–	–	–	–	–	–	–	–	–	–
TI	5–60	6	15	32	30	17	0	–	–	–	–	–	–	–	–	–	–	–	–	–	–	–
	10–50	0	0	0	0	0	4	11	27	33	17	8	–	–	–	–	–	–	–	–	–	–
	10–60	0	0	1	1	3	9	13	30	25	12	6	–	–	–	–	–	–	–	–	–	–
	15–60	0	0	0	0	0	0	0	0	0	4	4	15	30	24	20	3	–	–	–	–	–
	20–60	1	0	0	0	0	0	0	0	0	0	0	0	0	3	6	13	24	24	18	10	1
	2–30	41	49	0	–	–	–	–	–	–	–	–	–	–	–	–	–	–	–	–	–	–
	3–45	16	48	35	1	–	–	–	–	–	–	–	–	–	–	–	–	–	–	–	–	–
	5–30	3	13	21	23	36	4	–	–	–	–	–	–	–	–	–	–	–	–	–	–	–
	5–50	3	12	31	37	17	0	–	–	–	–	–	–	–	–	–	–	–	–	–	–	–
WI	5–60	3	10	29	41	17	0	–	–	–	–	–	–	–	–	–	–	–	–	–	–	–
	10–50	0	0	0	1	1	1	12	24	34	23	4	–	–	–	–	–	–	–	–	–	–
	10–60	0	0	1	0	1	7	13	19	31	27	1	–	–	–	–	–	–	–	–	–	–
	15–60	0	0	0	0	0	0	1	0	0	2	5	8	31	28	22	3	–	–	–	–	–
	20–60	0	0	0	0	0	0	0	0	0	0	0	0	0	0	4	12	21	34	17	9	3

Table A4. Simulation fraction of ejections (per cent) considering the gas lifetime of 5 Myr.

	Sim.	Number of ejected embryos																				
	ID	0	1	2	3	4	5	6	7	8	9	10	11	12	13	14	15	16	17	18	19	20
	2–30	50.0	48.7	1.3	–	–	–	–	–	–	–	–	–	–	–	–	–	–	–	–	–	–
	3–45	19.7	50.8	28.1	1.4	–	–	–	–	–	–	–	–	–	–	–	–	–	–	–	–	–
	5–30	1.7	11.0	23.1	32.9	29.2	1.9	–	–	–	–	–	–	–	–	–	–	–	–	–	–	–
	5–50	1.7	14.2	29.9	36.8	16.4	1.0	–	–	–	–	–	–	–	–	–	–	–	–	–	–	–
TI	5–60	2.4	11.6	30.2	36.4	18.4	1.0	–	–	–	–	–	–	–	–	–	–	–	–	–	–	–
	10–50	0.0	0.1	0.4	0.4	1.1	12.0	22.2	33.9	23.4	0.8	0.0	–	–	–	–	–	–	–	–	–	–
	10–60	0.0	0.1	0.2	0.9	1.2	5.4	13.3	26.1	31.3	1.1	0.0	–	–	–	–	–	–	–	–	–	–
	15–60	0.0	0.0	0.0	0.0	0.0	0.0	0.2	0.1	0.2	0.9	7.7	16.3	29.2	3.7	14.1	0.6	–	–	–	–	–
	20–60	0.0	0.0	0.0	0.0	0.0	0.0	0.0	0.0	0.0	0.0	0.0	0.0	0.3	1.0	2.5	9.6	18.7	27.4	26.0	13.3	1.2
	2–30	55.1	44.0	0.9	–	–	–	–	–	–	–	–	–	–	–	–	–	–	–	–	–	–
	3–45	28.6	50.2	20.3	0.9	–	–	–	–	–	–	–	–	–	–	–	–	–	–	–	–	–
	5–30	2.8	9.0	27.2	39.1	18.5	3.4	–	–	–	–	–	–	–	–	–	–	–	–	–	–	–
	5–50	4.1	17.3	33.8	28.1	12.2	4.5	–	–	–	–	–	–	–	–	–	–	–	–	–	–	–
WI	5–60	5.8	19.8	31.9	29.8	10.2	2.5	–	–	–	–	–	–	–	–	–	–	–	–	–	–	–
	10–50	0.0	0.0	0.1	0.4	1.9	6.6	16.5	29.8	28.9	13.3	2.5	–	–	–	–	–	–	–	–	–	–
	10–60	0.0	0.2	0.2	0.6	2.2	7.4	17.0	27.3	31.7	11.3	2.1	–	–	–	–	–	–	–	–	–	–
	15–60	0.0	0.0	0.0	0.0	0.0	0.1	0.0	0.3	0.8	3.5	11.4	19.2	27.5	24.9	10.2	2.1	–	–	–	–	–
	20–60	0.0	0.0	0.0	0.0	0.0	0.0	0.0	0.0	0.0	0.0	0.0	0.3	0.9	3.0	5.8	9.3	23.3	28.1	19.5	8.5	1.3

Downloaded from https://academic.oup.com/mnras/article/526/3/4435/7291961 by guest on 24 October 2023

Table A5. Simulation fraction of ejections (per cent) considering the gas lifetime of 9 Myr.

	Sim. ID	Number of ejected embryos 0	1	2	3	4	5	6	7	8	9	10	11	12	13	14	15	16	17	18	19	20
	2–30	46	54	0	–	–	–	–	–	–	–	–	–	–	–	–	–	–	–	–	–	–
	3–45	24	52	23	1	–	–	–	–	–	–	–	–	–	–	–	–	–	–	–	–	–
	5–30	2	8	24	34	27	5	–	–	–	–	–	–	–	–	–	–	–	–	–	–	–
	5–50	7	14	33	32	11	3	–	–	–	–	–	–	–	–	–	–	–	–	–	–	–
TI	5–60	4	23	38	15	15	5	–	–	–	–	–	–	–	–	–	–	–	–	–	–	–
	10–50	0	0	0	2	2	8	15	32	27	12	2	–	–	–	–	–	–	–	–	–	–
	10–60	0	0	0	0	4	10	17	24	32	11	2	–	–	–	–	–	–	–	–	–	–
	15–60	0	0	0	0	0	0	0	1	3	2	6	15	32	26	13	2	–	–	–	–	–
	20–60	0	0	0	0	0	0	0	0	0	0	0	0	0	3	3	9	16	32	22	12	3
	2–30	43	55	2	–	–	–	–	–	–	–	–	–	–	–	–	–	–	–	–	–	–
	3–45	23	53	24	0	–	–	–	–	–	–	–	–	–	–	–	–	–	–	–	–	–
	5–30	2	9	20	41	28	0	–	–	–	–	–	–	–	–	–	–	–	–	–	–	–
	5–50	1	16	35	37	10	1	–	–	–	–	–	–	–	–	–	–	–	–	–	–	–
WI	5–60	2	14	43	27	14	0	–	–	–	–	–	–	–	–	–	–	–	–	–	–	–
	10–50	0	0	0	0	1	6	10	31	30	22	0	–	–	–	–	–	–	–	–	–	–
	10–60	0	0	0	3	3	4	13	27	31	17	2	–	–	–	–	–	–	–	–	–	–
	15–60	0	0	0	0	0	0	0	0	0	2	6	12	26	29	23	6	–	–	–	–	–
	20–60	0	0	0	0	0	0	0	0	0	0	0	0	1	1	3	6	11	29	31	17	1

Table A6. Number of close encounters with Jupiter.

Gas Lifetime	Sim. ID	Number of CE TI	Number of CE WI	CE/Sim.∗ TI	CE/Sim.∗ WI	CE/Sim./Emb.∗∗ TI	CE/Sim./Emb.∗∗ WI
	2–30	13139	16038	131.39	160.38	65.70	80.19
	3–45	54989	70993	549.89	709.93	183.30	236.64
	5–30	193122	175475	1931.22	1754.75	386.24	350.95
	5–50	126594	119028	1265.94	1190.28	253.19	238.06
2 Myr	5–60	96675	121372	966.75	1213.72	193.35	242.74
	10–50	314433	268866	3144.33	2688.66	314.43	268.87
	10–60	284017	239499	2840.17	2394.99	284.02	239.50
	15–60	358930	361309	3589.30	3613.09	239.29	240.87
	20–60	487454	397843	4874.54	3978.43	243.73	198.92
	2–30	31748	23665	317.48	236.65	158.74	118.33
	3–45	64533	81892	645.33	818.92	215.11	272.97
	5–30	155400	157013	1554.00	1570.13	310.80	314.03
	5–50	136396	128970	1363.96	1289.70	272.79	257.94
3 Myr	5–60	132914	100916	1329.14	1009.16	265.83	201.83
	10–50	280848	271936	2808.48	2719.36	280.85	271.94
	10–60	234505	255878	2345.05	2558.78	234.51	255.88
	15–60	452541	306065	4525.41	3060.65	301.69	204.04
	20–60	478130	410823	4781.30	4108.23	239.07	205.41
	2–30	252616	302588	252.62	302.59	126.31	151.29
	3–45	1790236	1715291	1790.24	1715.29	358.05	343.06
	5–30	679942	803610	679.94	803.61	226.65	267.87
	5–50	1376267	1428031	1376.27	1428.03	275.25	285.61
5 Myr	5–60	2688799	2279990	2688.80	2279.99	268.88	228.00
	10–50	1191812	1158561	1191.81	1158.56	238.36	231.71
	10–60	2334830	2223382	2334.83	2223.38	233.48	222.34
	15–60	3565645	3358231	3565.65	3358.23	237.71	223.88
	20–60	4598449	4305990	4598.45	4305.99	229.92	215.30
	2–30	27945	31932	279.45	319.32	139.73	159.66
	3–45	173728	164029	1737.28	1640.29	347.46	328.06
	5–30	62570	69332	625.70	693.32	208.57	231.11
	5–50	135203	109653	1352.03	1096.53	270.41	219.31
9 Myr	5–60	265642	224071	2656.42	2240.71	265.64	224.07
	10–50	116061	108673	1160.61	1086.73	232.12	217.35
	10–60	240555	218485	2405.55	2184.85	240.56	218.49
	15–60	345363	330376	3453.63	3303.76	230.24	220.25
	20–60	454653	395149	4546.53	3951.49	227.33	197.57

Note. ∗**CE/Sim** are the number of CE per simulation; ∗∗**CE/Sim./Emb.** are the number os CE per simulation per initial number of embryos in the simulation.

Downloaded from https://academic.oup.com/mnras/article/526/3/4435/7291961 by guest on 24 October 2023

Table A7. Fraction of simulations forming UN-analogues.

Gas Lifetime	Sim. ID	1 TI (per cent)	1 WI (per cent)	2 TI (per cent)	2 WI (per cent)	3 TI (per cent)	3 WI (per cent)
	2–30	18	24	82	75	00	00
	3–45	34	31	48	57	12	11
	5–30	30	26	01	03	00	00
	5–50	37	25	05	03	00	00
2 Myr	5–60	36	26	36	45	17	17
	10–50	05	05	02	00	00	00
	10–60	41	27	01	03	01	00
	15–60	02	02	00	00	00	00
	20–60	03	00	00	00	00	00
	2–30	54	49	30	41	00	00
	3–45	44	46	43	40	07	07
	5–30	39	39	02	02	00	00
	5–50	40	25	03	02	00	00
3 Myr	5–60	48	41	27	32	05	12
	10–50	11	04	00	00	00	00
	10–60	50	31	02	04	01	00
	15–60	12	03	00	00	00	00
	20–60	00	01	00	00	00	00
	2–30	44.0	48.7	43.1	42.8	–	–
	3–45	40.3	43.3	36.9	38.4	8.2	6.2
	5–30	39.9	32.2	2.2	2.3	0.0	0.0
	5–50	39.2	30.1	2.7	1.8	0.0	0.0
5 Myr	5–60	38.6	45.7	34.2	36.3	8.5	5.6
	10–50	10.7	4.4	0.0	0.1	0.0	0.0
	10–60	37.6	27.2	1.7	1.4	0.0	0.0
	15–60	8.7	3.1	0.1	0.0	0.0	0.0
	20–60	3.0	0.7	0.0	0.0	0.0	0.0
	2–30	54	55	41	41	–	–
	3–45	36	40	44	38	10	09
	5–30	42	31	01	01	00	00
	5–50	48	32	03	00	00	00
9 Myr	5–60	44	44	22	37	15	08
	10–50	15	04	00	00	00	00
	10–60	47	40	00	00	00	00
	15–60	11	04	00	00	00	00
	20–60	01	00	00	00	00	00

Note. We run 1000 simulations for each setup setting the gas lifetime of 5 Myr and 100 simulations for the setups using gas lifetime of 2, 3, and 9 Myr.

Downloaded from https://academic.oup.com/mnras/article/526/3/4435/7291961 by guest on 24 October 2023

Table A8. Number of simulations with 2–5 remaining embryos in which 1–3 UN-analogue were formed and the outermost embryo is equal or larger than the innermost one.

Gas	Sim.	2 Embryos $(E > I)$		3 Embryos $(E = M = I)$		3 Embryos $(E = M > I)$		3 Embryos $(E > M = I)$		3 Embryos $(E = I > M)$		4 Embryos $(E > all)$		5 Embryos $(E > all)$	
Lifetime	ID	TI	WI	TI	WI	TI	WI	TI	WI	TI	WI	TI	WI	TI	WI
	3–45	2	1	12	11	0	0	0	0	0	0	–	–	–	–
	5–30	0	3	0	0	0	0	0	1	0	0	0	0	0	0
	5–50	1	1	0	0	0	0	2	0	1	1	0	0	0	0
2 Myr	5–60	0	1	11	16	1	0	2	0	2	0	0	0	0	0
	10–50	0	0	0	0	0	0	0	0	0	0	0	0	0	0
	10–60	2	1	0	0	0	1	0	0	0	0	0	0	1	0
	15–60	1	0	0	0	0	0	0	0	0	0	0	0	0	0
	20–60	0	0	0	0	0	0	0	0	0	0	0	0	0	0
	3–45	3	0	7	7	0	0	0	0	0	0	–	–	–	–
	5–30	1	0	0	0	0	0	0	0	0	0	0	0	0	0
	5–50	0	3	0	0	0	0	0	0	0	0	0	0	0	0
3 Myr	5–60	0	0	5	12	0	0	0	0	0	0	0	0	0	0
	10–50	0	0	0	0	0	0	0	0	0	0	0	0	0	0
	10–60	3	1	1	0	1	0	0	0	0	0	0	0	0	0
	15–60	0	2	0	0	0	0	0	0	0	0	0	0	0	0
	20–60	0	0	0	0	0	0	0	0	0	0	0	0	0	0
	3–45	8	2	82	62	0	0	0	0	0	0	–	–	–	–
	5–30	13	7	0	4	0	1	0	1	0	0	1	5	0	0
	5–50	5	8	0	7	0	1	0	1	3	0	5	9	0	0
5 Myr	5–60	10	18	8	5	1	1	4	0	4	0	12	6	0	0
	10–50	10	9	0	0	1	0	1	0	1	0	12	5	0	1
	10–60	10	8	0	0	1	0	2	3	0	1	12	9	0	2
	15–60	9	7	0	0	0	0	1	0	1	0	21	15	1	1
	20–60	12	12	0	0	1	0	2	0	1	0	26	30	3	4
	3–45	1	3	10	9	0	0	0	0	0	0	–	–	–	–
	5–30	1	0	0	0	0	0	0	0	0	0	0	1	0	0
	5–50	1	1	0	0	0	0	0	1	0	0	1	1	0	0
9 Myr	5–60	0	2	3	8	0	0	0	0	0	0	0	2	1	1
	10–50	0	1	0	0	0	0	0	0	0	0	0	0	0	0
	10–60	3	0	0	0	0	0	0	0	0	0	1	4	0	0
	15–60	1	0	0	0	0	0	0	0	0	1	1	0	0	0
	20–60	4	0	0	0	0	0	0	0	0	0	2	0	0	0

Note. After Saturn, **E** represents the outermost embryo, **I** the innermost, and **M** the intermediate embryo. We count here simulations that formed at least 1 UN-analogue.

This paper has been typeset from a TEX/LATEX file prepared by the author.

© The Author(s) 2023.
Published by Oxford University Press on behalf of Royal Astronomical Society. This is an Open Access article distributed under the terms of the Creative Commons Attribution License (https://creativecommons.org/licenses/by/4.0/), which permits unrestricted reuse, distribution, and reproduction in any medium, provided the original work is properly cited.

Downloaded from https://academic.oup.com/mnras/article/526/3/4435/7291961 by guest on 24 October 2023